DISSERTATION

On

BOND GRAPH AIDED THERMAL ANALYSIS OF FINITE JOURNAL BEARING

Submitted in partial fulfilment of the requirement for the award of degree

of

Master of Engineering

IN

CAD/CAM Engineering

Submitted by

Shubham Choudhary

Roll No.: 801381020

Under the Supervision of

Dr. Tarun Kumar Bera

and

Dr. Anirban Bhattacharya

Department of Mechanical Engineering

Thapar University, Patiala

DEPARTMENT OF MECHANICAL ENGINEERING

THAPAR UNIVERSITY

PATIALA-147004, INDIA

JULY-2015

DECLARATION

I hereby declare that the thesis entitled "**Bond Graph Aided Thermal Analysis of Finite Journal Bearing**" is an authentic record of my study carried out as requirement for the award of the degree of **Master of Engineering** in **CAD/CAM Engineering** at **Thapar University, Patiala,** under the supervision of **Dr. Tarun Kumar Bera**, Associate Professor and **Dr. Anirban Bhattacharya,** Assistant Professor, Mechanical Engineering Department, Thapar University, Patiala. The matter embodied in this thesis has not been submitted to any other University or Institute for the award of any degree.

Shubham Choudhary

This is to certify that above statement made by the student is correct to the best of our knowledge and belief.

Dr. Tarun Kumar Bera 15/7/15
Associate Professor
Thapar University, Patiala

Dr. Anirban Bhattacharya 15/7/15
Assistant Professor
Thapar University, Patiala

Countersigned by:

Head of ME Department
Thapar University, Patiala

Dean of Academic Affairs
Thapar University, Patiala

ACKNOWLEDGEMENT

First, I would like to express my sincere and devoted gratitude to Dr. Tarun Kumar Bera, Associate Professor, Mechanical Engineering Department and Dr. Anirban Bhattacharya, Assistant Professor, Mechanical Engineering Department, Thapar University, Patiala for their continuous encouragement and guidance, without which this work couldn't have been completed. They supported me at every step throughout this work.

I would also like to thank Dr. S.K. Mohapatra, Senior Professor and Head, Mechanical Engineering Department, Thapar University, Patiala for his encouragement and inspiration for execution of the work.

I specially acknowledge Mr. Rajinder Kumar, Incharge Machine Shop, Mechanical Engineering Department, Thapar University, Patiala, for his generous support to use the workshop facilities for creating the experimental setup.

The generous and intellectual support of all the staff members of Mechanical Engineering Department is greatly appreciated. Finally, I would like to express my heartful thanks to my parents and friends for their help and best wishes for the successful completion of this work.

Above all, I express my indebtedness to the 'ALMIGHTY' for all his blessing and kindness.

Shubham Choudhary

Roll No. 801381020

ABSTRACT

Finite journal bearings are very common in different engineering fields. The load carrying capacity of the journal bearings are greatly dependent on the characteristics of the lubricant used, load acting on the journal, type of loadings, operating conditions. During service, the rise in temperature greatly influences the viscosity of the oil and thus reduces load bearing capacity. A good prediction of temperature rise at different loading and operating conditions could be helpful for the designers to safely predict the behaviour and load carrying capacity of the bearing. The objective of this research work is to determine the angular velocity, and linear velocity of rotor and temperature, viscosity, flow rate of the standard commercial lubricant for a finite journal bearing. For obtaining these results the experimental setup is fabricated and simulations are carried out using Bond Graph technique. The experimental setup consists of journal bearing arrangement with rotors, coupling, base plate, motors, thermocouples and temperature indicator. In this shaft-rotor system the static and dynamic loads are given with the help of rotors i.e. concentric rotors and eccentric rotors of different masses. Four rotors are used to analyze the variation of these parameters with respect to time at different journal speeds. These rotors give different results with different journal speed and simulation results are nearly equal. The system behavior shows that the journal stability is reached very quickly. Experimental results show the increase in temperature with increase in speed, and increase in load. Higher temperature rise is predicted as well as measured when eccentric loading are applied.

Keywords:

Bond graph simulation; Journal bearing; Static and dynamic loading; Temperature rise; Flow rate; Journal speed; Experimental validation

LIST OF ABBREVIATIONS

SAE	Society of Automotive Engineers
FEM	Finite Element Method
CFD	Computational Fluid Dynamics
C	Compliance Element
I	Inertial Element
R	Resistance Element
L	Inductor
GY	Gyrator
TF	Transformer
SE	Source of Effort
SF	Source of Flow
AISI	American Iron and Steel Institute
EN	European Norms

NOMENCLATURE

A	Exposed Surface Area of Housing
c	Bearing clearance
D	Diameter of the Bearing
D	Distance between Left Bearing to Right Bearing
e	Eccentricity
e_1	Rotor eccentricity
F_1	Shear forces of Beam
G	Acceleration due to Gravity
h	Combined Heat Transfer Coefficient
h_o	Fluid Film Thickness in Journal bearing
H_d	Heat Dissipated inside the Bearing
H_g	Heat Generated inside the Bearing
J_{xx}	Rotary inertia in x-direction
J_{yy}	Rotary inertia in y-direction
J_{zz}	Rotary inertia in z-direction
k_r	Element stiffness matrix of the beam
k_s	Stiffness of the Shaft
K	Stiffness of the beam
L	Length of the Bearing
m	Journal mass
M	Mass of the Rotor
M_1	Bending moments of the Beam
N	Journal Speed
P	Load acting on Bearing
P_x	Pressure in X-direction

P_y	Pressure in Y-direction
Q	Flow rate
R	Bearing Radius
R_e	Torsional damping offered by coupling between motor and rotor shaft
R_i	Internal damping of rotor
R_j	Radius of Journal
R_m	Damping coefficient of motor
R_r	Damping Coefficient of Rotor
R_s	Damping Coefficient of Shaft
S_p	Specific heat of oil
T	Final temperature
T_a	Surrounding Temperature of Air
T_i	Initial temperature
T_o	Average Oil Film Temperature
T_s	Surrounding Temperature of Housing
u_1	Velocity
V	Voltage
y_1	Displacement
α	Constant Value
γ	Coefficient Value
θ	Attitude angle
θ_1	Twisting Moments of the beam
μ	Coefficient of Friction
μ_o	Viscosity of the oil
ρ	Density of oil
τ_L	Torque

ω	Angular Velocity
ω_{m}	Constant Angular Velocity of motor

LIST OF FIGURES

LIST OF TABLES

TABLE OF CONTENTS

CHAPTER 1 INTRODUCTION

Hydrodynamic lubrication of journal bearing plays a vital role in heavy machineries at high operational speeds. The bearing supports another moving element due to pressure developed inside the journal bearing arrangement. Moreover, the main focus is on bearing performance characteristics that will help for carrying heavy loads and enhances the bearing life in running condition.

1.1 Background and motivation

In most cases, the machines operating at higher speed will fail after some time because the load carrying capacity of the bearing reduces and metal to metal contact seizes the system. In that case the whole system is shut down due to development of wear and tear action in the bearing and journal arrangement. The thermal characteristics and viscosity parameter of oil is the key factor to analyze the bearing performance characteristics.

So, the main objective of this work is to analyze the bearing temperature with viscosity at different journal speeds and varying loads.

1.2 Journal bearing

Bearing is a machine element whose function is to support an applied load by reducing friction between the relatively moving surfaces. Loads may be applied in any direction i.e. radially, axially and combination of these. If the bearing supports the radial load, it is called radial journal bearing as shown in Fig.1 (a) and (b).

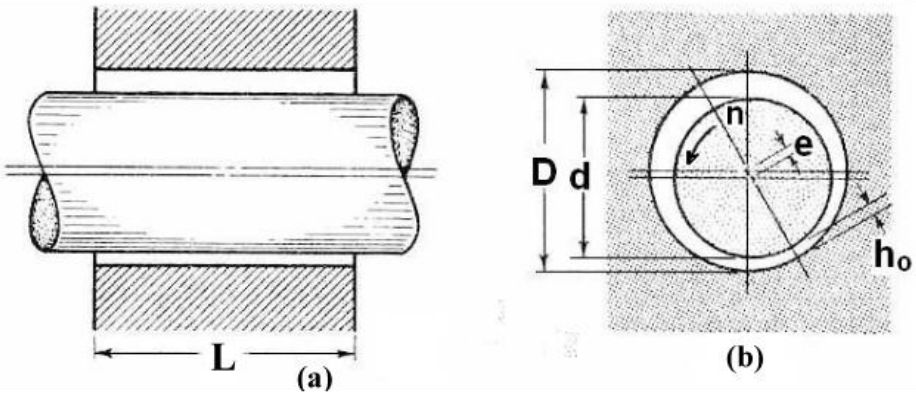

Fig. 1.1 Side and front view of radial journal bearing **[1]**

The journal bearing can be divided into full journal bearing where the contact angle between bush and bearing is 360° and the other is partial bearing where the contact angle is either 180° or less [**1**]. Full journal bearings are widely used in industry because these bearings can take up fluctuating loads. Partial bearings have limitations that they are used when direction of radial load is constant. The classified bearings are shown in Fig. 1.2.

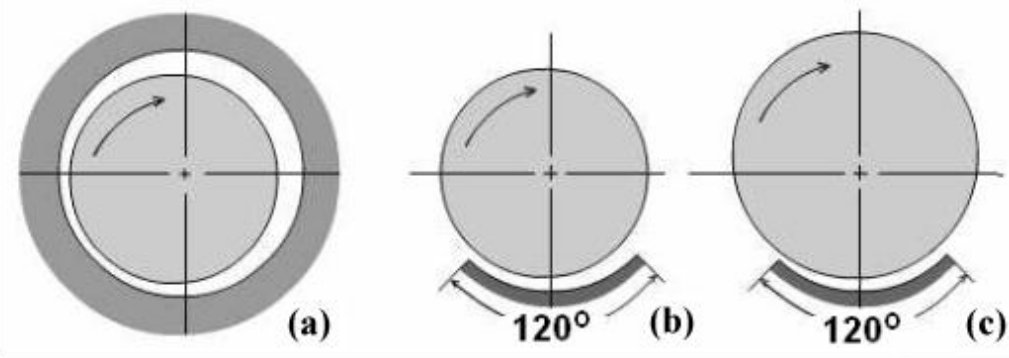

Fig. 1.2 Schematic diagram of (a) Full, (b) Partial and (c) Fitted journal bearings

1.2.1 *Theory of fluid film bearing*

The fluid film bearings are those bearing in which the mating surfaces are completely separated by the lubricant film during operating condition. Bearing operates under such kind of lubrication are fluid film bearings. If metal to metal contact is completely separated by the fluid film system, sometimes it is known as perfect lubrication system. The fluid film bearing are lubricated by the hydrodynamic flow which is generated by the relative surface motion and /or externally pressurized.

1.2.2 Classification or types of bearings

Bearings are classified according to the application of applied load if bearing supports a load in radial direction, it is called radial journal bearing. On the other side, if thrust load is supported, it is called thrust or axial bearing. Some bearings support both thrust and radial loads; they are known as conical bearing. There are mainly two types of bearing commonly used in industry which are as follows:

- Fluid film bearings
- Rolling-element bearings

Fluid film bearing: The thick film lubrication of bearing is divided into principal categories, mainly – (1) self-acting (2) externally-pressurized. Self-acting bearing generate pressure as a result of convergent film, relative motion of bearing, rotation of journal and speed of journal for externally pressurized bearing, pressurized lubricant is supplied by an external source and the lubricating film is maintained to carry the load. The bearings are also known as hybrid bearing as their operational principles including both self-acting and externally pressurization.

Rolling-element bearing: These bearings are widely used in industries as compare to the sliding bearing because rolling bearings have lower friction. The lubricant used in rolling-element bearings is usually grease.

1.2.3 Hydrodynamic theory of lubrications

In this operation, the black annulus represents the bushing or bearing element and the grey circle represents the shaft which is placed within oil film as shown in Fig.1.3. The shaft or journal carries a load *P* on it [**2**]. Here, journal diameter is smaller than the bush diameter and it will always rotate with an eccentricity.

When journal is at rest, it is seen from the Fig. 1.3 (a) due to the load *P*, the journal is in contact with bush element at the lower most position and there is no oil film between journal and bearing or bush. Now, journal starts rotating at low speed with acting load *P*, it has a tendency to shift to its side as shown in Fig. 1.3 (b). At the equilibrium position, the frictional force will balance the component of bearing loads. In order to achieve the equilibrium position, the journal or shaft orients itself with respect to the bearing element. Here, θ is the angle of friction. At higher speed operation the equilibrium position shifts and a continuous fluid film is created as shown in Fig. 1.3 (c). This continuous film has a converging zone or wedge zone, which is shown Fig. 1.3 (d) in the magnified view [**3**]. It has been observed that due to presence of wedge or converging zone the, the fluid film is capable of carrying heavy loads. It is necessary to build a positive pressure in continuous fluid film to supports heavy loads.

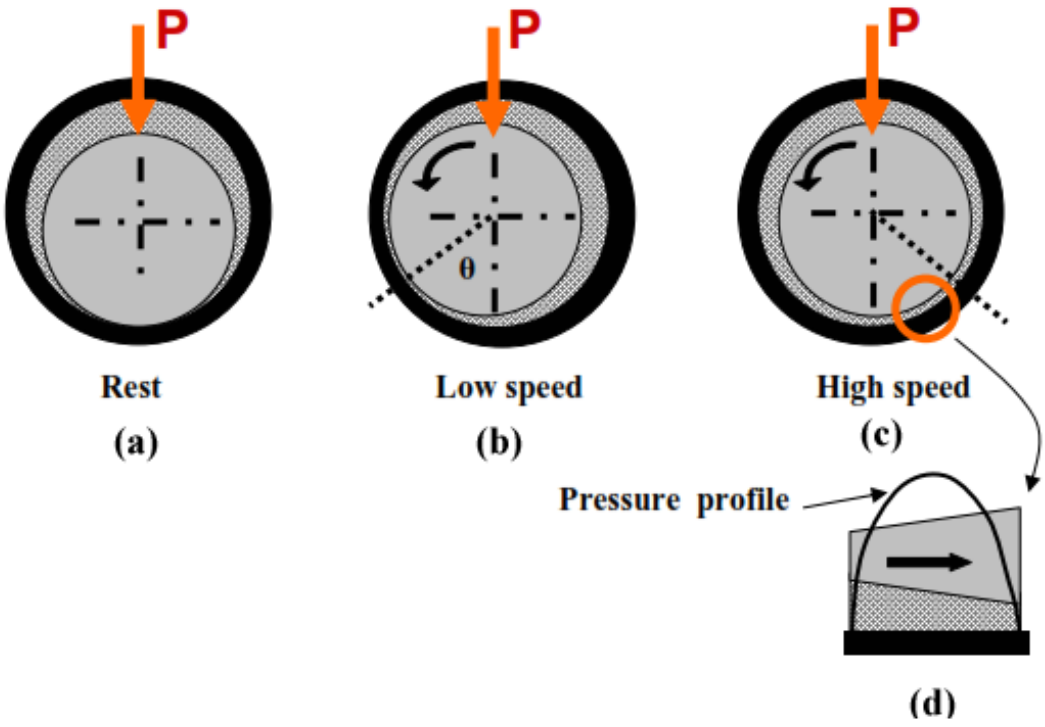

Fig. 1.3 Operation of journal bearing with hydrodynamic lubrications [**2**]

1.2.4 *Short and long journal bearing*

Journal bearing is further classified in three categories which are as follows:

- Short bearing
- Long bearing
- Square bearing

In short bearing, the *L*/*D* ratio is less than 1 which means diameter of the bearing is greater than the length of the bearing [**4**]. Here, let us assumed the *L*/*D* ratio is 0.5 the pressure gradient in y-direction $\frac{\partial P}{\partial Y}$ is the order of *P*/*L* and $\frac{\partial P}{\partial X}$ is the order of *P*/*D*. There are some conditions if *L*<*D* then *P*/*L*>*P*/*D*, so $\frac{\partial^2 P}{\partial X^2} << \frac{\partial^2 P}{\partial Y^2}$. X is the circumferential direction and Y is the is the radial direction. Therefore, Reynolds equation reduces to

$$\frac{\partial}{\partial Y}\left(h^3 \frac{\partial P}{\partial Y}\right) = 6\eta U \frac{\partial h}{\partial X} \tag{1.1}$$

The pressure equation is obtained by integrating the above equation twice with respect to *Y* and using the half Somerfield conditions.

In long bearing the *L*/*D* ratio is greater than 1 which means diameter of the bearing is less than the length of the bearing. Here, let us assumed the *L*/*D* ratio is 2 the pressure gradient in y-direction $\frac{\partial P}{\partial Y}$ is the order of P/L and $\frac{\partial P}{\partial X}$ is the order of *P*/*D*. There are some conditions if *L*>*D* then *P*/*L*<*P*/*D*, so $\frac{\partial^2 P}{\partial X^2} >> \frac{\partial^2 P}{\partial Y^2}$. Therefore, Reynolds equation reduces to

$$\frac{\partial}{\partial X}\left(h_O^3 \frac{\partial P}{\partial X}\right) = 6\eta U \frac{\partial h_O}{\partial X} \tag{1.2}$$

The pressure equation is obtained by integrating the above equation twice with respect to '*X*' and using the half Somerfield conditions. In square bearing the *L*/*D* ratio is 1 which means both length and diameter of the bearing are equal.

1.2.5 *Materials and oil used in bearings*

Bearing materials constitute an important part of any journal bearing. Its importance starts at the starting of the hydrodynamic lubrication where metal to metal contact occurs during operation. There are few desirable properties of a good bearing material which are as follows:

- It has a conformability and deformability property to sustain the local high pressures caused by shaft deflection and misalignment time.
- Indentation softness, which permit small particles to becomes safely indented in the material to protect the journal or shaft against wearing action.
- It has low shear strength for easy smoothing of the surface.
- Materials have adequate amount of compressive and fatigue strength for supporting the load.
- It should have good thermal conductivity to dissipate the frictional heat.
- It should have better corrosion resistance property against the lubricant and other combustion products like engine.

Composition of bearing materials: Babbit materials are most common used as bearing material. It have excellent property i.e. embeddability and conformability but have low fatigue and compressive strength [5]. Babbits can hardly use above 121℃. Other bearing materials such as aluminum bronze, tin bronze, copper lead alloy, cast iron etc. The widely used bearing material composition is as follows:

1. Tin-base babbits with 89% Sn, 8% Pb and 3% Cu,

2. Lead-base babbits with 75% Pb,15% Sb and 10% Sn,
3. Copper alloys such as Cu-10% to 15% Pb.

Lubricant: The clearance space of bearing a substance called lubricant is introduced. Any substance having some viscosity is known as lubricant. Mostly lubricants are used as cooling agent by carrying away heat generated by fluid friction in the system. Oils and greases are the most commonly used lubricants and by use of lubricant the energy lost by the friction is reduced. There are some properties of good lubricants are:

- It should adhere to the surface and reduce the wear.
- It should have good thermal and oxidative properties
- Is should carry away heat generated by the fluid friction
- It should protect system from noise, corrosion etc.
- It should have better cleaning effect on the surface
- It should be cheap and available in excess.

Recommended lubricants for journal bearing application as shown below:

1. SAE 10: Spindle oil for light loaded bearing and high speeds.
2. SAE 20-40: Machine oil for bearing of machine tools, IC engines, turbine etc.
3. SAE 40-50: Machine oil for diesel engine heavy loads and medium speeds.
4. SAE 60-70: Machine oil for high temperature, heavy load and low speeds.

1.2.6 *Heat generation and lubricant temperature*

The thermal aspect of hydrodynamic lubrication is the important consideration in design [**5**]. The temperature inside the bearing is effectively dissipated so that the equilibrium condition is reached in a very short time. Average temperature of the oil should not be exceeding 93 to 123℃ to prevent quick deterioration of oil.

The frictional heat generated can be calculated from the load *(P*), coefficient of friction (μ) and the journal speed (*N*).

$$V = \frac{2 \times \Pi \times N \times D}{60000} \tag{1.3}$$

Where, *N* is in rpm and *D* in mm

The frictional power loss:

$$H_g = P \times \mu \times V \tag{1.4}$$

Where H_g is expressed in Nm/s or W

Heat dissipated:

$$H_d = h \times A \times (T_s - T_a) \tag{1.5}$$

Where, H_d is expressed in Ns/m or W

h = combined heat transfer coefficient (convection and radiation), W/m^2 ℃

A = Exposed surface area of housing, m^2

T_s = Surrounding temperature of housing, ℃

T_a = Surrounding temperature of air, ℃

Here, the value of h depends on the geometry, material and roughness of the housing, temperature difference between housing and surrounding objects and temperature and velocity of the air. The similar expression can be written between temperature difference of housing and lubricant oil film as given below:

$$T_o - T_s = \alpha \times (T_s - T_a) \tag{1.6}$$

Where T_o is average oil film temperature and α is a constant depending upon lubrication system used. Combining these to equation and get finally expression:

$$H_d = h \times A \times B \times (T_o - T_a) \tag{1.7}$$

Where, $B = \dfrac{1}{(\alpha + 1)}$

1.3 Contribution of Thesis

The contribution of the thesis is as follows:

- The modelling is done for the rotor-shaft system with help of bond graph technique. This model is used to analyze or determines the variation in temperature, viscosity, flow rate, displacements and pressure with respect to time at different journal speeds.
- This modelling technique consists of Rayleigh's beam model, finite bearing model and thermal model. Basically, thermal model is to determine the temperature of lubricant inside the journal bearing arrangement.
- For validation of simulation results, the experimental setup is prepared.
- In the experimentation the whole set up is installed onto the plate where, the assembly of bearings, shaft with rotors, coupling and the motor torque is transmitted by the coupling to the system.

- Rotors are used for providing static and dynamic loads to the system i.e. rotor without eccentricity and rotor with eccentricity.

1.4 Organization of thesis

Thesis is organized in five chapters. The overview information including these chapters is as follows:

Chapter 1 includes the introduction part, journal bearing, fluid film theory, hydrodynamic lubrication, short and long bearings, materials and oil used and the heat generation and lubricant temperature.

Literature review related to the rotor dynamics, thermal modelling of journal bearing and bond graph modelling is included in Chapter 2. Other rotor dynamic systems are also given in the literature. The literature gap and objective of the thesis are also included in this chapter.

Chapter 3 includes the basic introduction of bond graph and its application in various other domains. This chapter also includes the modelling of shaft-rotor system in which the system description, bond graph modelling of finite journal bearing , modelling of Rayleigh's beam model and also included in simulation and parameter results.

Chapter 4 is experimentation of shaft-rotor system which includes introduction, selection of material and components used in the system like base plate, motor, shaft, bearings, coupling, rotors, thermocouple and temperature indicator. The explanation of system setup, experimentation and validation or comparison of results is also included in this chapter.

Chapter 5 includes conclusions and scope of future work.

CHAPTER 2 LITERATURE REVIEW

2.1 Introduction

In this chapter the literature review of rotor dynamics, thermal modelling and bond graph modelling of journal bearing is presented. This chapter consists of thermal modelling of journal bearing under different loading condition and bearing characteristic performance is discussed. The variation of viscosity and pressure phenomena with respect to temperature is presented. In this system the various strategies are implemented which illustrated at this chapter.

2.2 Rotor dynamics

The analysis of linear and rotary motion of the spinning rotor can be easily predicted by the Euler's and Newton's equation but sometimes, these equations creates problem to better understand of physical significance of the models [**6**]. This can be possible without writing any equations and analyze the behavior of dynamic system. The proper understanding of dynamic behaviors and related to their computational algorithms is easily predicted by bode diagram and Nyquist diagram.

A turbomachine's in rotor dynamic mostly emphasis on the characteristic behaviour of the system which means how its shaft will vibrate [**7**]. In rotor dynamic the two parameters are always in consideration i.e. resonance and instability and these are the common threat in every rotor dynamic system. This threat continued when industrial demands of high speed machinery, pressure and power levels. So, many design inspection can be performed usually in rotor dynamics considering the critical speed and instability. Inspection is also highly proposed for the machine rerates and any changes in the assembly of system, bearings, coupling, motor etc. The Modelling and design tools help to improve the rotor dynamic performance.

Rotor dynamic analysis is the important factor for the development of rotor bearing systems in order to secure the rotor instabilities, bearing overheating, whirling of shaft and other unwanted things [**8**]. To analyze the rotor dynamic behavior which is supported by the hydrodynamic bearing is the important parameter. The complexity level of the system is increased by visualizing the behavior of instability, bearing overheating etc. A Reynolds equation is used to determine the lubrication film pressure inside the journal bearing under different loading conditions. As the frequency varies the whirl nature of flexible shaft can easily

see. Design engineer enables to evaluate the rotor critical speed and bearing design criteria at very early stage of development.

The rotor is modelled by different method along with the shafts having their own weights and moment of inertia [**9**]. One of the methods is to determine the natural frequencies of the rotating system. The complete system is discretized in small element and develops ordinary differential equation in the matrix form. The bearings at the end of the shaft are modelled as equivalent spring and dampers which can determine by the boundary conditions in discretized manner. The gyroscopic effects is considering in the analysis of rotor-bearing system and thickness of the disk also be considered. The results shows that the stiffness of the shaft and the natural frequency of the system increases while the amplitude of vibration of the system decrease on account of increasing thickness of the bearing. The advantage of this method is to evaluate the conventional approximation by varying the thickness of disk and bearing size. This parameter has a considerable effect on the vibration behavior of the system and easily configure to rotor-bearing system.

Damping plays an important role in any mechanical system and the importance of dynamic system increases with increase of operational speed. As damping with higher speed create more difficulty in the vibration nature and changes the nature of rotation of the rotor system [**10**]. Few methods are used to analyze and minimize this problem and providing a feasible solution of any complicated system. Rotor dynamics interacts between the elastic and inertia properties of rotor-bearing in mechanical system. Bearing stiffness and damping factors are the important parameter which affects more in the rotor dynamic system. Design of hydrodynamic bearing is based on the effective properties of the bearing through which minimize the unbalance nature of the shaft in different operational speed. Various methods to analyze the unbalance response of the rotor and can be solved by using Finite element method and transfer matrix method. Whenever we are talking about rotor dynamics the important parameter is comes under consideration i.e. gyroscopic effect and some cases it will be neglected.

A continuum model is used to analyze the dynamic behavior of rotor-bearing system [**11**]. For analysis this model finite element method is used which help to easy understand of model in simpler way. This model emphasis on the oil-whip phenomena which is the major cause of failure of rotor bearing system.

The importance of rotor dynamics plays a vital role and its demand increasing for higher speed operations and high speed machines [**12**]. During high speed operation with damping complicates the nature of vibration. In rotor dynamics damping plays an important role near the resonant frequency. Damping changes the nature of rotation in rotor dynamic system. The FEM analysis gives the feasible solution and reduces the complexity of the model.

2.3 Thermal modelling of journal bearing

The thermal effect on hydrodynamic journal bearing is the important factor for bearing performance [**13**]. Most of the authors still working in this field to predict the behavior or the determines the thermal effect in various operating speeds and loading condition. They used various methods to improve the shaft stability, reduce power losses, flow pressure and minimizing the bearing temperature. The non-circular bearing is extensively used for high speed operations and due to this temperature increases inside the bearing and power losses occurs. To minimize these losses vibrational approach method is used and analyzes the behavior of bearing characteristics.

Journal bearings are designed to minimize the wear rate, power loss and providing high damping coefficient [**14**]. In the low speed operations metal to metal contact is generates excessive amount of power loss and wears rate. Due to this phenomenon temperature inside the bearing is increases highly so, eliminate this problem a concept of hydrodynamic-permanent-magnet hybrids of journal is introduced. In this concept the repulsive type passive magnet levitation used through which reduction in starting torque at low speed is achieved and the main advantage is to achieve low friction at medium and low speed in the single bearing arrangement. The experimental setup is also prepared to investigate the performance characteristics and temperature variation in the journal bearing.

In the modern industry the machineries rotating at high speed and high performance are used. The load carrying heavy rotor of modern industry is widely used for that hydrodynamic journal bearing is used [**15**]. When bearing operates on high speed the heat generation is more due to shearing action in the fluid film which raises its temperature inside the bearing at the expense of lower viscosity. This affects the performance characteristics of bearing and reduces the load carrying capacity. To realize this behavior and to obtain the realistic performance characteristic most of the analyst drives the two dimensional energy equations to find the temperature distribution in the fluid film. Furthermore researchers obtain the three dimensional

energy equation for temperature and pressure distribution in the fluid film by using CFD technique.

In thermo hydrodynamic the turbulent flow of lubricant is analyzed on the basis of computational fluid dynamics (CFD) [**16**]. Turbulence in the lubrication affects the performance characteristics of journal bearing. The numerical solution of Navier-Stokes equation which is having the kinetic energy of turbulence under the consideration of incompressible and steady flow is obtained. The cavitation effects are also be consider while using this approach and also prepared the cavitation model to analyze the cavitation inside the bearing. From this technique the velocity, pressure and temperature distribution in circumferential direction is obtained without using any approximation technique. The turbulence and cavitation model easily determines the pressure, velocity and temperature inside the journal bearing arrangement. When fluid is passed through the convergent region the maximum temperature is obtain at the vicinity of minimum film thickness after that the lubricant temperature reduces. This technique helps to easily prediction of pressure, velocity and temperature inside the journal bearing arrangement.

Analyzed the dynamic characteristics hydrodynamic journal bearings having finite width isotropic roughness affect Vsines concepts of stochastic process [**17**]. Based on the principle of isotopic roughness pattern (roughness is uniform by distributed over the bearing surface.), the rotor-dynamic coefficient have been evaluated following first order perturbation of the dynamic Reynolds type equation roughness effects on the dynamic response. Coefficients are observed for higher value of eccentricity ratio. Stability of bearings deteriorates with increasing roughness parameter, including stability for smother bearing surface.

Present some aspects of surface roughness in lubrication [**18**]. It is shown that uniform roughness structure tends to result in a lower load capacity, a higher load capacity, a higher lubricant in flow and a higher friction mainly depends on the shear stress while load may still be carried mainly by hydrodynamic.

The bearing characteristics play an important role for the performance of the bearing [**19**]. The journal bearing test rig is performed for different operating condition like SAE20W40 oil is used under 300 N and 450 N applied force at range of 1500 rpm to 1750 rpm. Then, records the temperature and pressure variation and analyze the same characteristics with other oils used like vegetable oils, rapeseed oil and soya bean oil.

Hydrodynamic journal bearing supports and guide the rotating shafts of high-speed components [**20**]. Manufacturing defects creates the major problem in the thermal distortions in the running condition such as misalignment problem. Such destructive effects can be justified to development of numerical model for easy prediction of bearing characteristics under steady state conditions.

A comparative study of load carrying capacity and pressure distribution of journal bearing is analytically solved by various methods [**21**]. Sometime, in the analysis of load carrying capacity and pressure distribution the thermal effect are also considered. Moreover, the effects of variations in operating loading condition which minimize the efficiency rate of the journal bearing. Such cases, the analytical results and finite element results are compared to analyze the fluctuation of the behavior.

The thermo hydrodynamic performance is analyzed by creating microgroove on the shaft [**22**]. A journal bearing is modelled by the CFD technique and equations are solved. The effect induced by a microgroove is dependent on the depth of groove, eccentricity and different bearing configurations. The microgroove produces a drop of pressure due to which load carrying capacity is reduced.

2.4 Bond graph modelling of journal bearing

Bond graph is the powerful tool to represent or explain any system which has energy in different domains [**23**]. This technique is used in every domain and any system. The modelling city traffic is also be modelled by using the probabilistic model and queuing theory with mathematical representation. The concept of city traffic model involves all dynamics that will exist in real - time traffic. In this concept of traffic flow is very undistributed to analyze this problem bond graph is used for easy understanding.

In the rotor dynamic system the gyroscopic effect is very crucial to understand the nature of the system. The equation of motion of generalized rotor motor system is derived by the Lagrange's approach with consideration of gyroscopic effects [**24**]. Bond graph technique helps to minimize the complexity of the system and visualize the rotor dynamic phenomena from visual perspectives. This can derives all necessary equation of motion and state space equation without any difficulty. In the design of high speed rotating system main focus is on critical speed, rotor's natural frequency, stability and steady state response of the system. Although the

complexity of the system varies as related factor is used to analyses. This technique gives the appropriate result and easily modelled any system.

The modelling of rotating machine and simulation like motors, generators etc. can easily done by bond graph technique [**25**]. They are widely used in industry to derive any system at different operational speed. During operational condition huge amount of power losses occurs which reduces the efficiency of the system so as to study the behavior of such machines bond graph modelling technique is used. Bond graph modelling technique easily develop model to the feature of adaptability of the machine.

The study of squeeze film in rotor-bearing system using Newtonian and viscoelastic lubricants is different from other study [**26**]. In this system dynamic concept is analyzed by the bond graph modeling technique which helps to improve the stability range by using Newtonian fluid. Experimental setup is conducted for the comparison of theoretical studies. Newtonian fluid is squeezed in various operational speeds and analyzes the variation of temperature and pressure in the system to improve bearing characteristics. This modelling technique helps for better understanding and generates the ordinary differential equations of the system.

2.5 Literature Gap

After detailed studies of literature on journal bearing, it was observed that most of the research was done on the performance characteristics of the bearing. The bearing carries various loads under different loading conditions due to which various parameters like pressure, temperature, velocity, viscosity, *etc* are changing. To analyses these parameter various studies was done by researchers to improve the bearing life and performance in running condition. In recent researches the main focus is to predict the efficiency of the bearing using different lubricants. As per our survey very little work is done on viscosity parameter which is extensively affected by the temperature variation. So our research work will be on analysis of viscosity of oil with respect to temperature variation under static and dynamic loading condition. The bearing is designed for particular viscosity at maximum motor speed to carry the loads and supports the moving element. Our research work will helps for designer to design bearing under different loading conditions.

2.6 Objective of work

According to the literature survey the bearing performance characteristic is the key factor for improving the efficiency of the system. The objective of the work and summarized points are as follows:

- Bond graph model is prepared for the analysis of viscosity, thermal variation, discharge, linear and angular velocity of rotor.
- Model consists of finite bearing model, Rayleigh's beam model and thermal modelling.
- The experimental setup is prepared for the validation of simulation results and results are validated with simulation results.
- This main objective is that whenever, bearing is design the viscosity of the fluid is the main deciding factor for load carrying capacity.
- When bearing works under heavy loads and high speed operation, the temperature inside the bearing is very high which reduces the viscosity of oil and reduces the pressure.
- When pressure decreases the load carrying capacity of the bearing also decreases and there are chances for metal to metal contact which seize the motion of the system and may be wear and tear occurs.
- To avoid this problem our objective is to analyze the pressure, viscosity and temperature variation occurs under static and dynamic loading condition in the rotor-shaft system.
- The bond graph modelling technique is used for modelling the thermal system and results simulation is done by giving specified parameters of the system.

CHAPTER 3 THERMAL MODELLING OF FINITE JOURNAL BEARING

3.1 Introduction

The dynamical equations of the system are obtained by the Reynolds equations with half Sommerfeld boundary conditions. For obtaining the differential equations, Reynolds equations are solved. The equations are solved by the numerical techniques. It takes more time when these differential equations are solved manually. So, the requirement of such a technique which can generates and solves the differential equation in very short interval of time. This is possible by using the bond graph modelling technique. Bond graph itself develops the differential equation by modelling the system. In this chapter, this technique is used to develop the thermal model of journal bearing at different motor speed.

3.2 Bond graph modelling

In 1959, Prof. H. M. Paynter of MIT was developed the modelling technique with the help of basic elements. This idea works on the basis of seven elements i.e. inertial element (I), compliance element (C), resistive element (R), source of effort (SE), source of flow (SF), transformer (TF) and gyrator (GY). All elements have different characteristic representation and property of the system. Through these elements the information convey to the system and after conveying the information, the computer is automatically generates the differential equations. Bond graph also works in various systems like mechanical, electrical, thermal, hydraulic, *etc*. Other elements for electrical and mechanical systems are damper, mass, spring, capacitor, inductor, resistor *etc*. These basic elements help to solve and understand the whole system in very simpler manner.

These elements directly interacts each other by mean of power or energy. This power or energy is in the form of flow or effort. The flow variable and the effort variable for different system are shown in Table 3.1.

Table 3.1: Power variables in different energy domains

Systems	Efforts (*e*)	Flow (*f*)
Mechanical	Force (N)	Velocity (m/s)
	Torque (Nm)	Angular velocity (rad/s)
Electrical	Voltage (V)	Current (A)
Thermal	Temperature (K)	Entropy change rate (W/K)
	Pressure (N/m^2)	Volume change rate (m^3/s)
Hydraulic	Pressure (N/m^2)	Volume flow rate (m^3/s)
Chemical	Chemical potential (Nm/mol)	Mass flow rate (mol/s)
	Entropy (Q/K)	Mass flow rate (kg/s)
Magnetic	Magnetic-motive force (AT)	Magnetic flux rate (Wb/s)

3.2.1 *Bond* graph *standard elements*

The basic elements which are used in representation of bond graph as I, C, R, SE and SF. The line segment called bond through which all elements are connected to each other [**27**]. This bonds carries the power i.e., effort information and flow information.

Bond graph model can be classified are as follows:

- Single port passive elements i.e. inertia (I), capacitance (C) and resistance (R).
- Active source elements i.e. source of effort (SE) and source of flow (SF).
- Two port conversion elements i.e. gyrator (GY) and transformer (TF).
- Junction elements i.e. flow summing junction (0) and effort summing junction (1).

3.2.2 *Basic 1-port element*

Single port elements having only one power port and every port consisting of single pair of effort and flow variable. There are two types of ports i.e., basic port and active port

In bond graph inertial element is called as inductor, compliance as capacitor and resistor as dashpot. They are called passive elements because they are not giving any power to the system.

- *Compliance element:* The compliance element is represented by a character 'C'. This bond is further connected to the rest of the system. The bond which is connected to the element carries the effort and the flow information. This device stores the energy and

imparts to the system. The integral causality is only preferable. The graphical representation of compliant element as shown in Fig. 3.1.

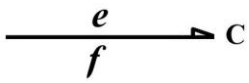

Fig. 3.1 Bond graph representation of compliance element

$$F = k.x \tag{3.1}$$

$$e = k.Q \tag{3.2}$$

$$e = k\int_{-\infty}^{t} f(t)dt \tag{3.3}$$

This gives integral causality and is preferable.

- *Inertial element:* This element gives the relationship between the effort and the flow in such a way that the integration of effort gives the flow. For mechanical system mass (m), polar moment of inertia (J) is used. For electrical system inductor (L) is used. The graphical representation of inertial element is shown in Fig. 3.2.

Fig. 3.2 Bond graph representation of inertial element

$$\text{Effort } F = m\ddot{x} = \frac{df}{dt} \times \text{ m} \tag{3.4}$$

$$f = \frac{1}{m}\int_{-\infty}^{t} edt \tag{3.5}$$

$$= \text{k} + \frac{1}{m}\int_{-\infty}^{t} edt \tag{3.6}$$

This equation gives the integral causality and it is preferable.

- *Resistive element:* Resistive element imparts the energy or power of the system in multi-dimensional system. It takes energy and delivers to the surrounding. This element represents by the character ‘R’ with a bond ahead of it. The bond carries both effort and

the flow information. The arrow is pointing towards the resistive element (R), which means power. The graphical representation of resistive element as shown in Fig 3.3.

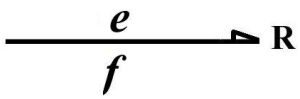

Fig. 3.3 Bond graph representation of resistive element

- *Source of effort:* Source of effort determines the effort with bond ahead of it. It gives effort to the system and it can be represented by the symbol 'SE' with a bond ahead of it. The example of source of effort in mechanical system is force. The graphical representation is shown below.

Fig. 3.4 Bond graph representation of source of effort element

- *Source of flow:* The Source of flow gives the flow to system and it is represented by the symbol of 'SF'. The example of source of flow in mechanical system is cam. During rotation of cam it will give the reciprocating motion of piston. The representation of source of flow as shown in Fig. 3.5.

Fig. 3.5 Bond graph representation of source of flow element

3.2.3 *Basic 2 -port element*

The basic 2-port elements are transformer and the gyrator. The symbolic representation of transformer is TF and gyrator is GY. Both elements have flow and effort information associated with the system. They have two bonds on each side which helps to transfer the information to system or from the system.

- *Transformer:* Transformer does not create nor destroys energy it magnifies the energy or magnitude. It conserves the power or receives from the system and then it deliver with a modified scaling factor. In transformer both the bonds having effort and flow information on each side. It converts flow to flow and effort to effort information after multiplying by

the scaling factor which magnifies the flow information and effort information. Transformer requires the direction of flow through which information is defined of the system.

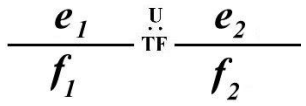

Fig. 3.6 Bond graph representation of transformer element

$$f_2 = \mu f_1 \tag{3.6}$$

$$e_1 f_1 = e_2 f_2 \tag{3.7}$$

$$\therefore e_2 = \frac{1}{\mu} e_1 \tag{3.8}$$

- *Gyrator:* Gyrator provides a relationship between flow to effort and effort to flow keeping powers same on both the ports. In gyrator there is no requirement of directions of flow.

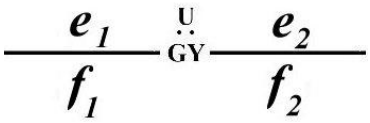

Fig. 3.7 Bond graph representation of gyrator element

$$e_2 = \mu f_1 \tag{3.9}$$

$$e_1 f_1 = e_2 f_2 \tag{3.10}$$

$$e_1 = \mu f_2 \tag{3.11}$$

3.3 Modelling of rotor-shaft system

The rotor-shaft system consists of rotors i.e. larger rotor with eccentricity or without eccentricity and smaller rotor with eccentricity or without eccentricity. These rotors are mounted on the journal shaft and providing static and dynamic loads at running condition. Bearing supports the journal or shaft and due to friction pressure, temperature varies according to the loading and journal speed. The whole system is explained by the bond graph technique which helps to

generate the ordinary differential equation and develop graphical representation of temperature of oil with respect to time.

3.3.1 *System description*

The system works on different journal speeds and loading conditions. The arrangement of rotor-shaft system (shown in Fig. 3.8) is mounted on the base plate which is further clamped on the rigid surface i.e. milling machine. Clamping of base plate is required to avoid vibration and tries to complete conversion of motor energy into the system. For smooth running between journal and bearing arrangement lubrication is used which helps to minimize the friction rate. During running condition there is development of pressure inside the bearing and temperature of oil raises which effect on viscosity of oil. The viscosity of oil decreases as temperature increases. So, in system description the analysis of temperature and viscosity of the oil at different loads and journal speeds is done.

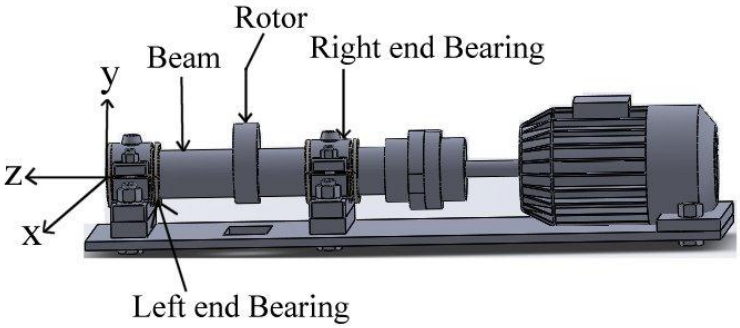

Fig. 3.8 Schematic representation of the rotor-shaft system

3.3.2 *Bond* graph *modelling*

Modelling of system consists of rotor-shaft system, Rayleigh's beam model, and infinite journal bearing. These models help for complete understanding of rotor shaft system. Bond graph generates the ordinary differential equation which helps to easy understanding regarding to the system. Bond graph modelling also generates the graphical representation by giving the system parameter values and initial condition if any.

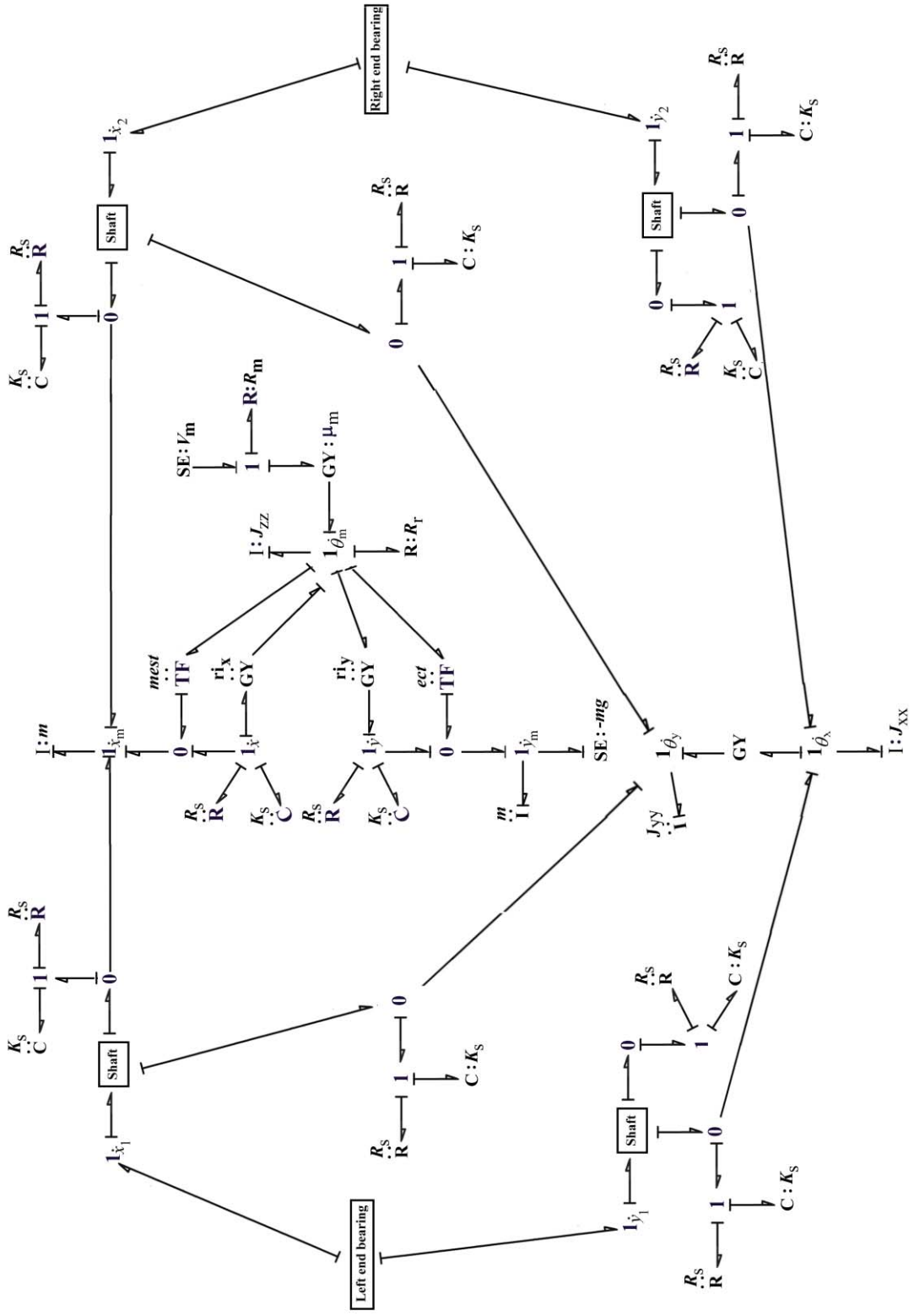

Fig. 3.9 Bond graph modelling of rotor-saft

Bond graph is one of helpful technique for a system modelling especially where different subsystems of a main system reside in different energy domain (like combination of mechanical and electrical energy, *etc*.) It is the unified approach (I , C , R , SE , SF ,TF , GY) through which any system can easily modelled. From this technique the ordinary differential equation can be generated automatically. Bond graph is modular in nature and any dynamic system can be modelled by bond graph technique. This technique consists of various systems (like Mechanical, Electrical, Hydraulic, Thermal, Chemical, Magnetic). Through all these system mechanical, electrical, hydraulic and thermal systems are discussed here. The bond graph of journal bearing arrangement as shown in Fig. 3.9. The voltage (v_m) input to the electrical dc motor which is denoted by SE-element (source of effort) connected at the 1-junction that defines equality of current throughout the junction. This may be noted that in bond graph modelling a 1-junction means summation of efforts equal to zero (like in mechanical system force and torque, electrical system voltage, hydraulic system pressure, thermal temperature and pressure, *etc*.) and flows are equal. In 1-junction only one flow input and inertia element is always connected with 1-junction only. Whereas, in 0-junction the summation of flows equal to zero (like in mechanical system velocity and angular velocity, electrical system current and voltage flow rate, hydraulic volume flow rate, thermal system entropy change rate and volume change rate *etc*.). The element connected at the same 1 junction is resistance (R_m). This is the electric part of the motor. The voltage is given to the resistance and the output i.e. current from R element is converted into the torque by a gyrator (GY) element. Gyrator elements convert flow to effort or vice versa. The rotary inertia (J_{zz}) of the disc and viscous damping (R_r) are presented by I and R element, respectively. The same flow is multiplied by transformer (TF) and the output gives flow at 1-junction.

On the other side, left end bearing elements gives source of flow (SF) at 1-junction here; source of flow is the velocity in X- direction of the journal. This flow transferred to the beam and then beams returns two type of flow or output i.e. linear and rotary flows. The structural stiffness of the beam gives an effort output to the disc connected at the centre at 0-junction . Similar, effect is observed to the right end of the bearing.

The mass which receives linear effort from the bearing gives flow as output at 1-junction. This flow is combines to that comes from the motor to obtain a resultant flow at 0-junction. This resultant flow through gyrator provides additional torque to the disc at 1- junction.

The whole process occurs in *x* and *y* direction simultaneously. The related equation of rotor-shaft system is as follows [**28**]:

$$u_1 = \omega R_j \tag{3.12}$$

Where, u_1= Velocity (m/s), ω = Angular velocity (rad/s) and R_j = Radius of journal (m)

$$Q = u_1 L e \tag{3.13}$$

Where, Q = Flow rate (m^3/s), L = Bearing length (m), e = Eccentricity (m)

$$F = \frac{2\mu_O \Pi R_j u_1 L}{c} \tag{3.14}$$

Where, F = Force acting on a bearing in (N), μ_o = Viscosity of the oil (Ns/m^2) and c = Bearing clearance (m)

$$T = T_i + \frac{0.8 F u_1}{\rho Q S_p} \tag{3.15}$$

Where T = Final temperature in (℃), T_i = Initial temperature (℃), ρ = Density of oil (Kg/m^3) and S_p = Specific heat of oil (J/K)

The coordinates of mass centre of disc are as follows [**29**]:

$$x_m = x + e\cos(\theta + \varphi) \tag{3.16}$$

$$y_m = y + e\sin(\theta + \varphi) \tag{3.17}$$

Where θ is the rotation of motor, e is the eccentricity and φ is the constant phase. The velocity relations are as follows:

$$\dot{x}_m = \dot{x} - e\dot{\theta}\sin(\theta + \varphi) \tag{3.18}$$

$$\dot{y}_m = \dot{y} + e\dot{\theta}\cos(\theta + \varphi) \tag{3.19}$$

Equation of motion of rotor shaft system

$$m\ddot{x} + (R_e + R_i)\dot{x} + R_i\dot{\theta}y + Kx = me\dot{\theta}^2\cos(\theta + \varphi) + me\sin(\theta + \varphi)\ddot{\theta} \tag{3.20}$$

$$m\ddot{y} + (R_e + R_i)\dot{y} - R_i\dot{\theta}x + Ky = me\dot{\theta}^2\sin(\theta + \varphi) - me\cos(\theta + \varphi)\ddot{\theta} \tag{3.21}$$

$$I_r\ddot{\theta} + R_r\dot{\theta} = R_c(\omega_m - \dot{\theta}) - \tau_L \tag{3.22}$$

Where I_r = External torsional damping

R_r = Rotary inertia of rotor-shaft system

ω_m = Constant motor speed

R_e = Torsional damping offered by coupling between motor and rotor shaft

τ_L = Torque

3.3.3 *Modelling of finite journal bearing*

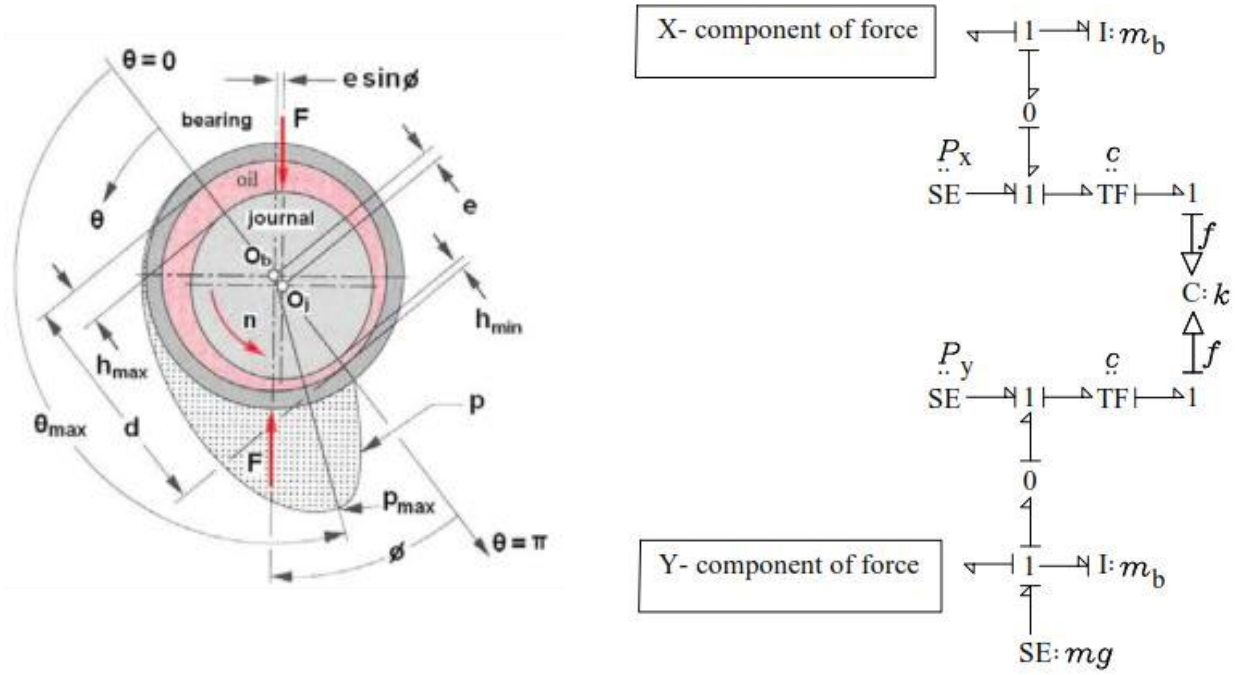

(a) (b)

Fig. 3.10 (a) Schematic representation [**30**] and (b) bond graph modelling of finite journal bearing

The finite bearing arrangement as shown in Fig. 3.10 the x- component of force gives effort at 1-junction. This effort converting into a flow by I element (mass of bearing). This flow directly goes to 1-junction through 0-junction. Due to which pressure is develop in x-direction because of rotation of journal into the bearing which is an effort at 1-junction. This effort is converted into flow by 0-junction and further multiplied by transformer (TF) value i.e. clearance between journal bearing which give flow output at 1-junction. This flow is measured by flow sensor (f). The same process occurs in y-direction also.

$$\in = \sqrt{\frac{x^2 + y^2}{c}} \tag{3.23}$$

Where, ϵ = eccentricity ratio and c is the bearing clearance in (m).

$$d \in = \frac{xdx + ydy}{\in c^2} \tag{3.24}$$

$$d\phi = \frac{ydx - xdy}{(\in c)^2} \tag{3.25}$$

$$\gamma = \frac{0.5\mu_O RL^2}{c^2} \tag{3.26}$$

Υ = coefficient value, μ_o = Viscosity of the oil (Ns/m^2), R = Bearing radius (m), L = Bearing length (m)

$$\theta = \tan^{-1}\left(\frac{2d \in}{\in(\omega - 2d\phi)}\right) \tag{3.27}$$

θ is the attitude angle and

$$\theta_2 = \theta + \prod \tag{3.28}$$

$$\xi = \sqrt{1 - \in^2} \tag{3.29}$$

$$\phi_1 = \tan^{-1}\left(\frac{\xi \sin\theta}{\cos\theta + \in}\right) \tag{3.30}$$

$$\phi_2 = \tan^{-1}\left(\frac{\xi \sin\theta_2}{\cos\theta_2 + \in}\right) \tag{3.31}$$

$$F_1 = \frac{f_1}{\xi^5} \tag{3.32}$$

$$F_2 = \frac{f_2}{\xi^4} \tag{3.33}$$

$$F_3 = \frac{f_3}{\xi^3} \tag{3.34}$$

$$P_1 = \gamma\left((\omega - 2d\phi) \in F_2 - 2d \in F_1\right) \tag{3.35}$$

$$P_1 = \gamma\left((\omega - 2d\phi) \in F_3 - 2d \in F_2\right) \tag{3.36}$$

$$P_x = \frac{P_2 y}{\in c} + \frac{P_1 x}{\in c} \tag{3.37}$$

$$P_y = \frac{P_2 x}{\in c} + \frac{P_1 y}{\in c} \tag{3.38}$$

Where, P_x = Pressure in X-direction (N/m^2) and P_y = Pressure in Y-direction (N/m^2)

3.3.1 *Modelling of Rayleigh's beam model*

In this model shaft divides into equal elements and each element is used to analyze. The element is having two degree of freedom i.e. linear velocity and angular velocity at each node means 4 degree of freedom of a single element of the shaft [**31**]. The stiffness of the beam element relates to the Newtonian forces to the generalized displacement at the end of the element as shown in Eq. 3.39.

$$\begin{Bmatrix} F_1 \\ M_1 \\ F_2 \\ M_2 \end{Bmatrix} = [K_r] \begin{Bmatrix} y_1 \\ \theta_1 \\ y_2 \\ \theta_2 \end{Bmatrix} \tag{3.39}$$

Here, F_1 and M_1 are the shear forces and bending moments at single node of the element. Similarly, same forces acting on another node. Here, y_1 and θ_1 are displacements and twisting moments of the beam. The stiffness matrix (K_r) is the compliance element which is attached to the C element. The value of element stiffness matrix is given in Eq. 3.40 and the Rayleigh's beam model as shown in Fig. 3.11.

$$[K_r] = \frac{EI}{l^3} \begin{bmatrix} 12 & 6l & -12 & 6l \\ 6l & 4l^2 & -6l & 2l^2 \\ -12 & -6l & 12 & -6l \\ 6l & 2l^2 & -6l & 4l^2 \end{bmatrix} \tag{3.40}$$

Where, K_r = Element stiffness matrix

EI= Flexural rigidity, l = Length of element

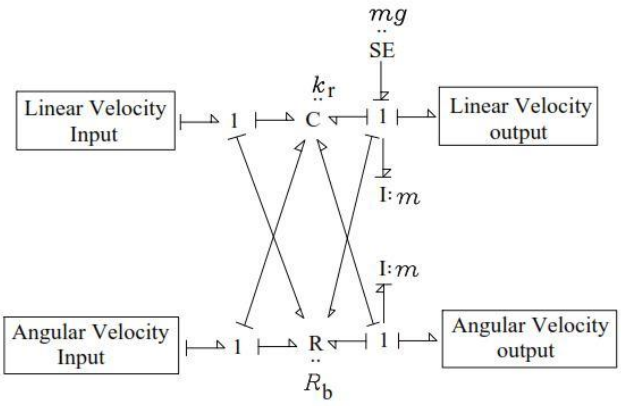

Fig. 3.11 Bond graph modelling of Rayleigh's beam model

The modelling of beam consists of five Rayleigh beam model. The complete beam is dividing into five elements and we already explain Rayleigh beam model in previous modelling. In this model the source of flow (SF) is taken as zero because shaft is fixed at one end. This complete beam model is the combination of these 5 elements as shown in Fig.3.12.

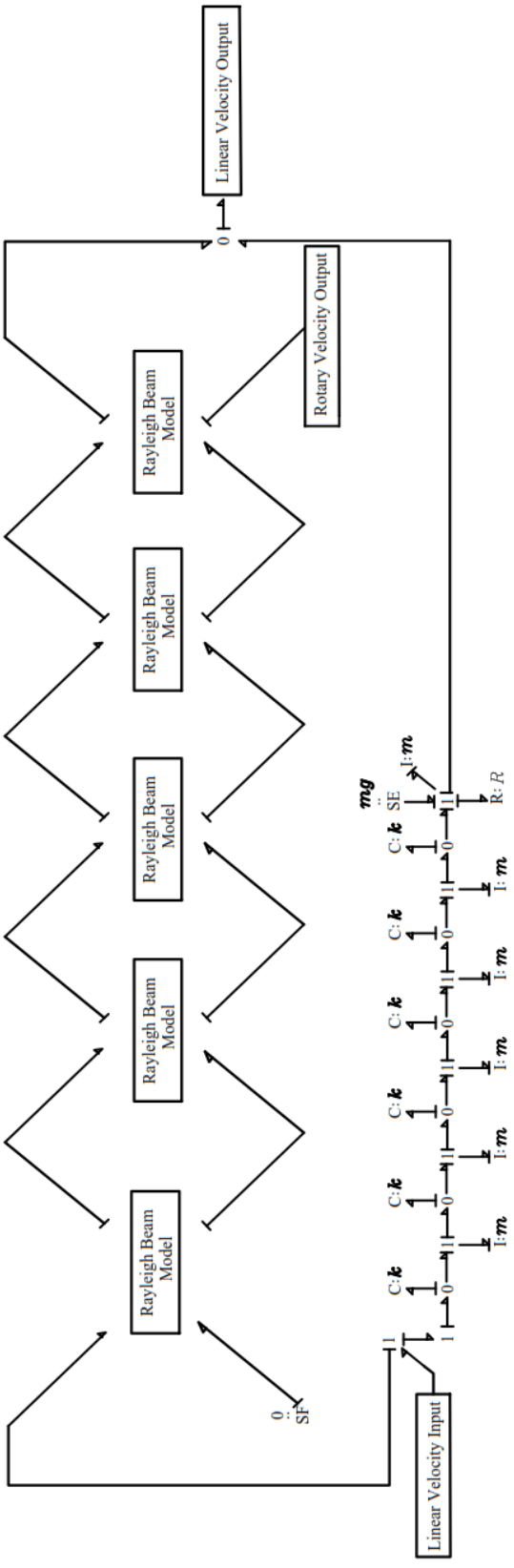

Fig. 3.12 Bond graph modelling of beam consisting of Rayleigh's beam model

3.6 Parameter values and simulation results of larger rotor without eccentricity

3.6.1 *Parameter values of larger rotor without eccentricity*

The parameter values of larger rotor without eccentricity as shown in Table 3.2

Table 3.2: Parameter values of larger rotor without eccentricity

Parameter	Values	Description
K_s	1×10^{6} N/m	Stiffness of the shaft
R_s	1×10^{2} Ns/m	Damping coefficient of shaft
c	1.1×10^{-4} m	Radial clearance of the bearing
N	200, 300, 400, 500, 600, 700, 800, 900, 1000 rpm	Journal speeds
T_i	22.7, 31.6, 25.6, 24.6, 28.6, 25.2, 29.4, 27.2, 28.8 K	Initial temperatures
e	5.016×10^{-6} m	Eccentricity
S_p	1800 J/K	Specific heat of the oil
L	0.0327 m	Bearing Length
ρ	872.5 kg/m^3	Density of the oil
R	0.01575 m	Journal radius
G	9.81 m/s^2	Acceleration due to gravity
m	1.57 kg	Journal mass
M	1.274 kg	Mass of the disc
J_{xx}	0.1 kgm^2	Rotary inertia in x-direction
J_{yy}	0.1 kgm^2	Rotary inertia in y-direction
J_{zz}	0.2 kgm^2	Rotary inertia in z-direction
D	0.115 m	Distance between left bearing to right bearing
R_r	2 Ns/m	Damping coefficient of motor
μ	5	Constant value
R_m	1 Ns/m	Damping coefficient of motor
V	113.1, 169.65, 226.2, 282.75,	Voltage

	339.3, 395.85, 452.4, 500.95, 565.5 V	
R_e	15 Ns/m	External damping of rotor
R_i	5 Ns/m	Internal damping of rotor
e_1	0 m	Rotor eccentricity
K	1×10^6 N/m	Stiffness of the rotor

All parameters values are same except initial temperature (T_i), Voltage (V) and Eccentricity (e) these parameter values are changing according to journal speeds and loads.

3.6.2 *Simulation results of larger rotor without eccentricity*

The variation in angular velocity with respect to time at different voltages are given Table 3.3

Table 3.3: Journal (or motor) angular velocity at different motor speed

Rpm	200	300	400	500	600	700	800	900	1000
Rad/s	20.94	31.4166	41.889	52.3611	62.833	73.3185	83.778	94.526	104.704

In this result the angular velocity of journal or shaft increasing with increase of time as shown in Fig. 3.13. As the journal rotates at higher motor speed the input voltage also increases with respect to time.

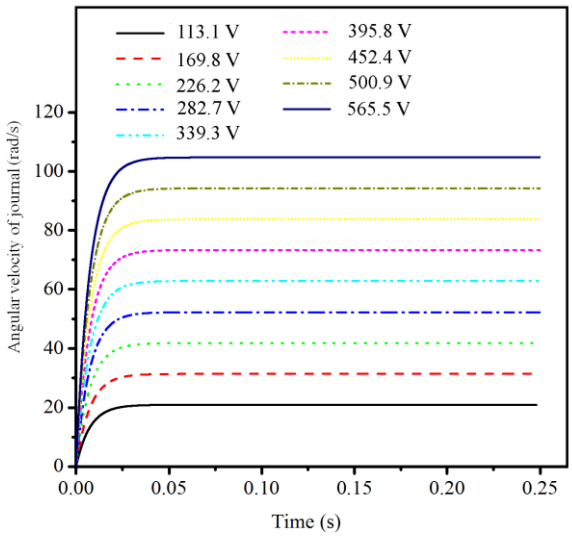

Fig. 3.13 Journal (or motor) angular velocity vs. time at input voltage for larger rotor without eccentricity

The linear velocity is also increasing with increase of time as shown in Fig. 3.14. At 200 rpm the linear velocity is 0.3275 m/s and after that it will constant throughout. At 300 rpm the linear velocity is 0.49135 m/s and after that it will constant throughout. At 400 rpm the linear velocity is 0.655142 m/s and after that it will constant throughout. At 500 rpm the linear velocity is 0.81892 m/s and after that it will constant throughout. At 600 rpm the linear velocity is 0.982731 m/s and after that it will constant throughout. At 700 rpm the linear velocity is 1.14678 m/s and after that it will constant throughout. At 800 rpm the linear velocity is 1.31028 m/s and after that it will constant throughout. At 900 rpm the linear velocity is 1.47407 m/s and after that it will constant throughout. At 1000 rpm the linear velocity is 1.638145 m/s and after that it will constant throughout.

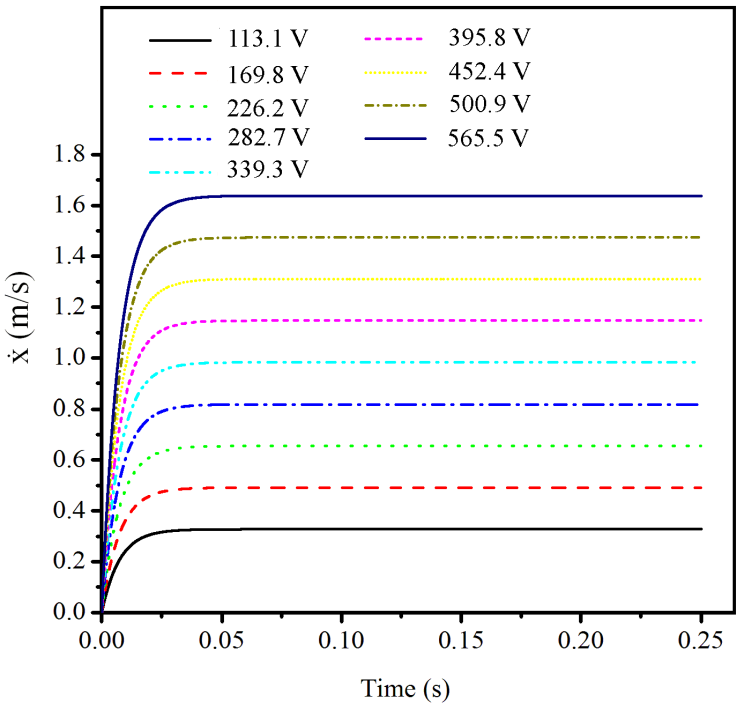

Fig. 3.14 Linear velocity vs. time variation of larger rotor without eccentricity

In this simulation result the circumferential flow is directly proportional to the journal speed. As the journal speed increases the flow inside the bearing also increases due to which temperature inside the bearing raise and creates a thin film layer as shown below.

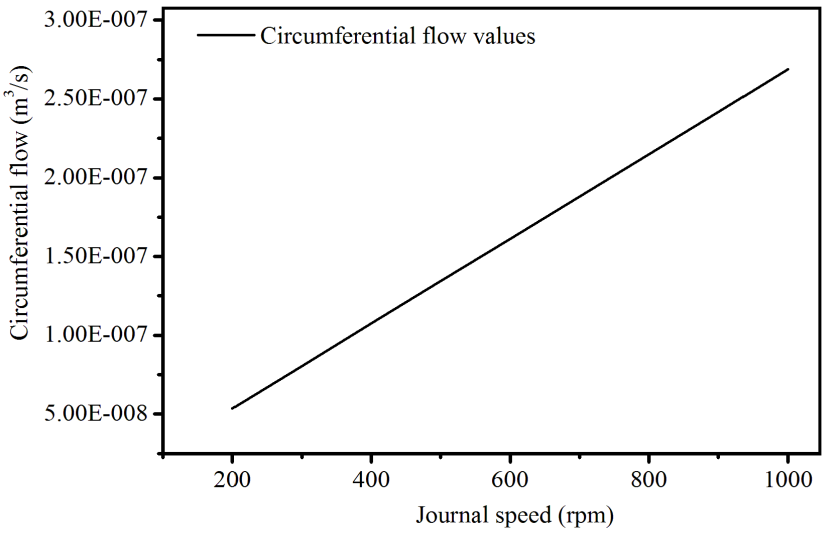

Fig. 3.15 Circumferential flow vs. journal speed variation of larger rotor without eccentricity

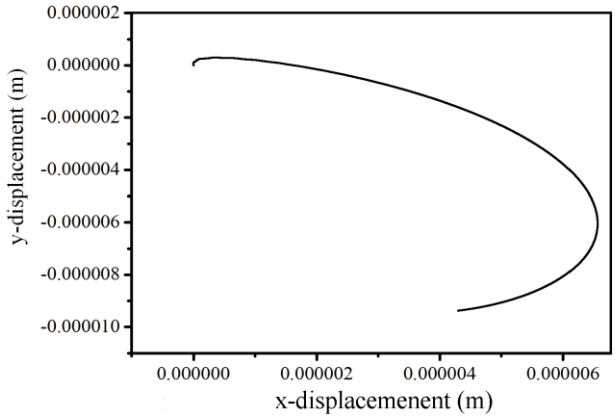

(a) 200 rpm, left bearing

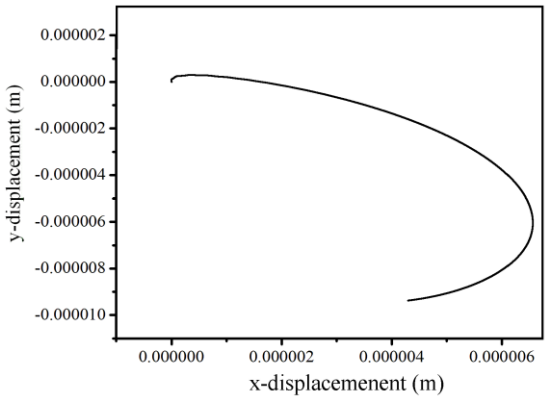

(b) 200 rpm, right bearing

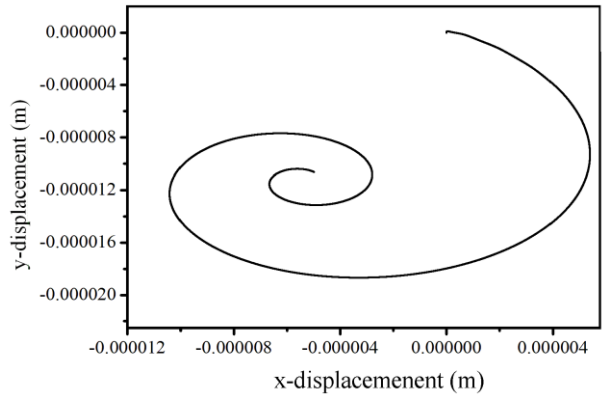

(c) 1000 rpm, left bearing

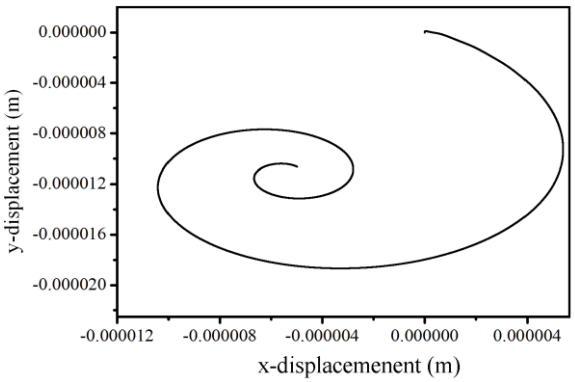

(d) 1000 rpm, right bearing

Fig. 3.16 Displacements in x and y direction of larger rotor without eccentricity

3.6.3 *Parameter values of larger rotor with eccentricity*

The parameter values of larger rotor with eccentricity as shown in Table 3.4

Table 3.4: Parameter values of larger rotor with eccentricity

Parameter	Values	Description
K_s	1×10^{6} N/m	Stiffness of the shaft
R_s	1×10^{2} Ns/m	Damping coefficient of shaft
c	1.1×10^{-4} m	Radial clearance of the bearing
N	200, 300, 400, 500, 600 rpm	Journal speeds
T_i	25, 25.1, 35.3, 31.4, 32.4 K	Initial temperatures
e	5.016×10^{-6} m	Eccentricity
S_p	1800 J/K	Specific heat of the oil
L	0.0327 m	Bearing Length
ρ	872.5 kg/m^3	Density of the oil
R	0.01575 m	Journal radius
G	9.81 m/s^2	Acceleration due to gravity
m	1.5839 kg	Journal mass
M	1.301 kg	Mass of the disc
J_{xx}	0.1 kgm^2	Rotary inertia in x-direction
J_{yy}	0.1 kgm^2	Rotary inertia in y-direction
J_{zz}	0.2 kgm^2	Rotary inertia in z-direction
L	0.115 m	Distance between left bearing to right bearing
R_r	2 Ns/m	Damping coefficient of motor
μ	5	Constant value
R_m	1 Ns/m	Damping coefficient of motor
V	113.1, 169.65, 226.2, 282.75, 339.3 V	Voltage
R_e	15 Ns/m	External damping of rotor
R_i	5 Ns/m	Internal damping of rotor

e_1	0.01 m	Rotor eccentricity
K	1×10^6 N/m	Stiffness of the shaft of rotor

All parameters values are same except initial temperature (T_i), Voltage (V) and Eccentricity (e) these parameter values are changing according to journal speeds and loads.

3.6.4 *Simulation results of larger rotor with eccentricity*

Table 3.5: Journal (or motor) angular velocity at different motor speed

rpm	200	300	400	500	600
rad/sec	23.346	29.328	42.580	52.93	60.986

In this result the angular velocity of journal or shaft increasing with increase of time. As the journal rotates at higher motor speed the input voltage also increases with respect to time.

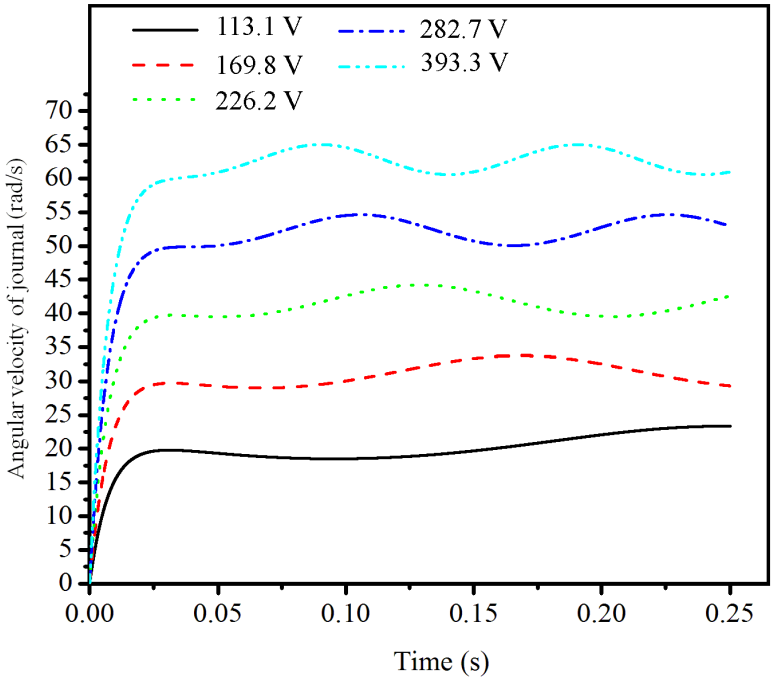

Fig. 3.17 Journal (or motor) angular velocity vs. time at input voltage for larger rotor with eccentricity

The linear velocity is also increasing with increase of time. At 200 rpm the linear velocity is 0.365141 m/s and after that it will constant throughout. At 300 rpm the linear velocity is 0.458694 m/s and after that it will constant throughout. At 400 rpm the linear velocity is

0.665961 m/s and after that it will constant throughout. At 500 rpm the linear velocity is 0.827861 m/s and after that it will constant throughout. At 600 rpm the linear velocity is 0.953783 m/s and after that it will constant throughout.

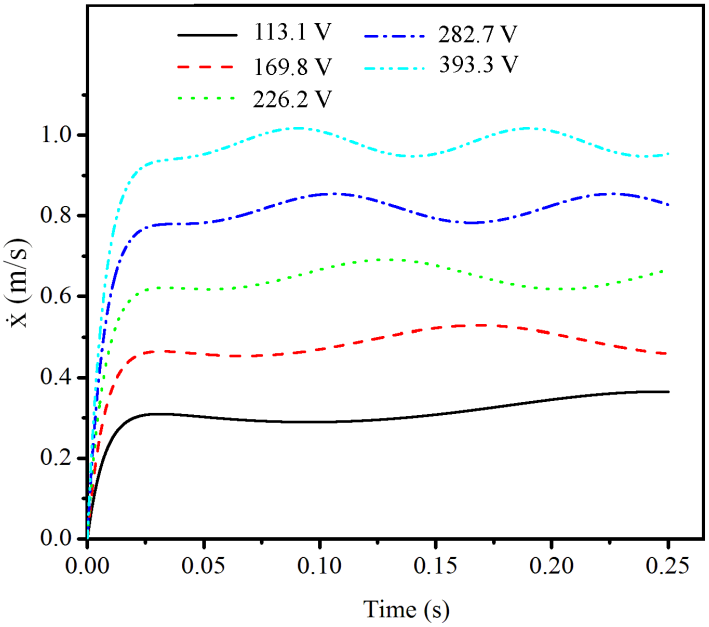

Fig. 3.18 Linear velocity vs. time variation of larger rotor with eccentricity

In this simulation result the circumferential flow is directly proportional to the journal speed. As the journal speed increases the flow inside the bearing also increases due to which temperature inside the bearing raise and creates a thin film layer.

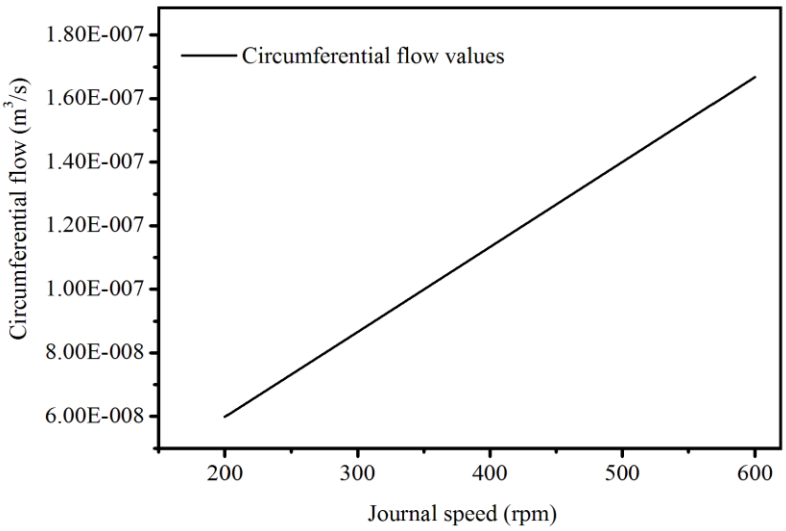

Fig. 3.19 Circumferential flow vs. journal speed variation of larger rotor with eccentricity

The displacement in x and y direction are shown in Fig. 3.19 when rotor rotates about shaft axis it will displace in x and y direction because of centrifugal force acting outwards. Due to centrifugal force rotor displace from the centroidal axis and gives displacement in x and y direction

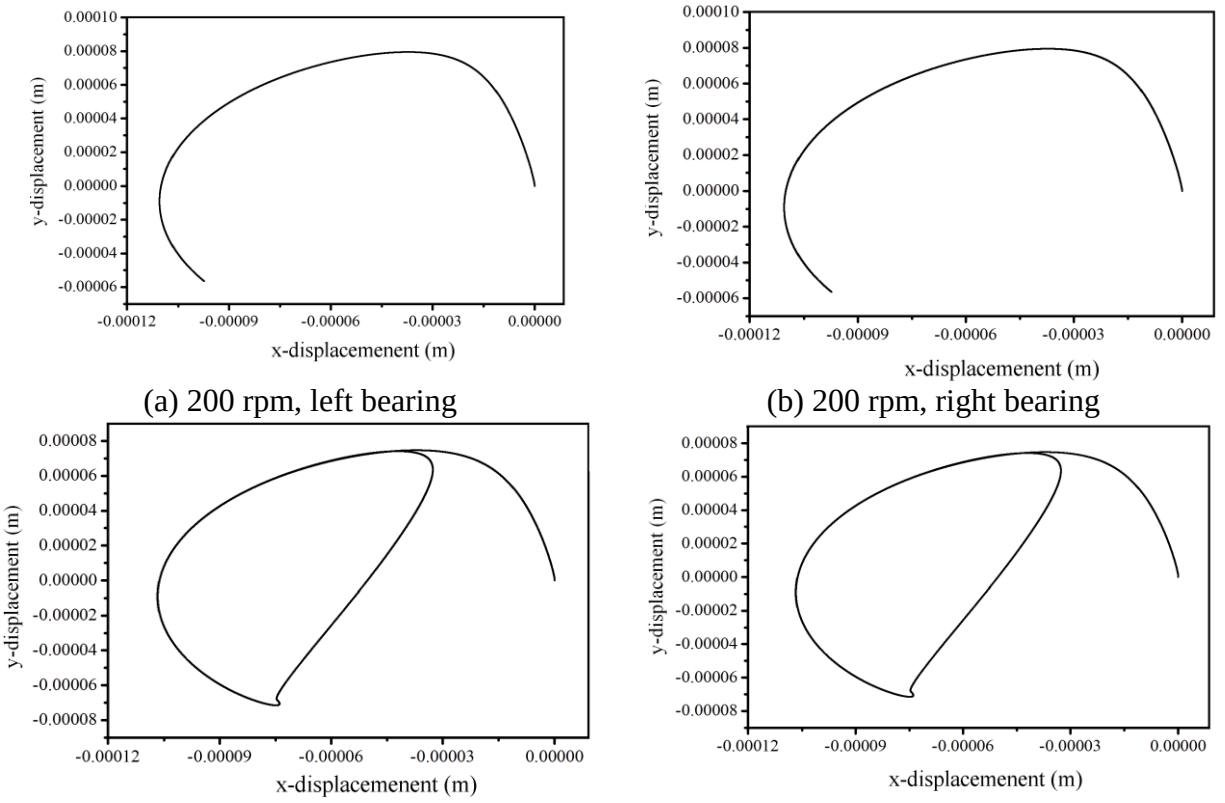

(a) 200 rpm, left bearing (b) 200 rpm, right bearing

(c) 600 rpm, left bearing (d) 600 rpm, right bearing

Fig. 3.20 Displacements in x and y direction of larger rotor with eccentricity

3.6.5 *Parameter values of smaller rotor without eccentricity*

The parameter values of smaller rotor without eccentricity as shown in Table 3.6

Table 3.6: Parameter values of smaller rotor without eccentricity

Parameter	Values	Description
K_s	1×10^{6} N/m	Stiffness of the shaft
R_s	1×10^{2} Ns/m	Damping coefficient of shaft
c	1.1×10^{-4} m	Radial clearance of the bearing
N	200, 300, 400, 500, 600, 700, 1000, 1250, 1500, 1750 rpm	Journal speeds
T_i	27.4, 23.4, 27.7, 27.6, 34.3, 33.6, 35.4, 29.5, 23, 24.2 K	Initial temperatures
e	5.016×10^{-6} m	Eccentricity
S_p	1800 J/K	Specific heat of the oil
L	0.0327 m	Bearing Length
ρ	872.5 kg/m^3	Density of the oil
R	0.01575 m	Journal radius
G	9.81 m/s^2	Acceleration due to gravity
m	1.2439 kg	Journal mass
M	0.621 kg	Mass of the disc
J_{xx}	0.1 kgm^2	Rotary inertia in x-direction
J_{yy}	0.1 kgm^2	Rotary inertia in y-direction
J_{zz}	0.2 kgm^2	Rotary inertia in z-direction
L	0.115 m	Distance between left bearing to right bearing
R_r	2 Ns/m	Damping coefficient of motor
μ	5	Constant value
R_m	1 Ns/m	Damping coefficient of motor
V	113.1, 169.65, 226.2, 282.75, 339.3,	Voltage

	395.85, 565.5, 706.875, 848.25, 989.625 V	
R_e	15 Ns/m	External damping of rotor
R_i	5 Ns/m	Internal damping of rotor
e_1	0 m	Rotor eccentricity
K	1×10^6 N/m	Stiffness of the rotor

All parameters values are same except initial temperature (T_i), Voltage (V) and Eccentricity (e) these parameter values are changing according to journal speeds and loads.

3.6.6 *Simulation results of smaller rotor without eccentricity*

Table 3.7: Journal (or motor) angular velocity at different motor speed

Rpm	200	300	400	500	600	700	1000	1250	1500	1750
Rad/s	20.944	31.4166	41.88	52.36	62.833	73.318	104.74	130.925	157.11	183.26

In this result the angular velocity of journal or shaft increasing with increase of time. In this result the angular velocity of journal or shaft increasing with increase of time. As the journal rotates at higher motor speed the input voltage also increases with respect to time.

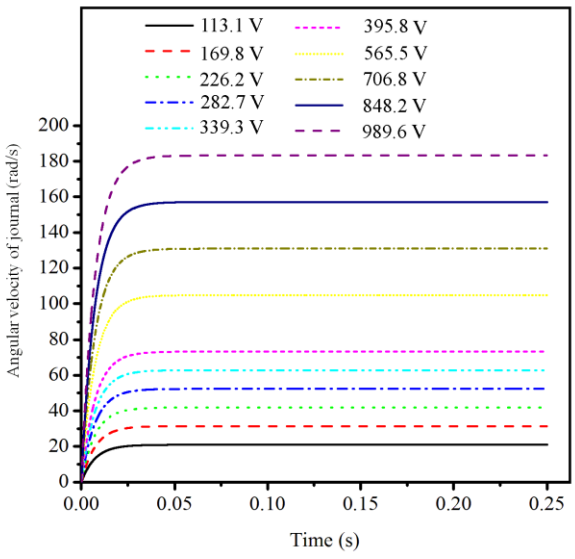

Fig. 3.21 Journal (or motor) angular velocity vs. time at input voltage for smaller rotor without eccentricity

The linear velocity is also increasing with increase of time. At 200 rpm the linear velocity is 0.3275 m/s and after that it will constant throughout. At 300 rpm the linear velocity is 0.49135 m/s and after that it will constant throughout. At 400 rpm the linear velocity is 0.655142 m/s and after that it will constant throughout. At 500 rpm the linear velocity is 0.81892 m/s and after that it will constant throughout. At 600 rpm the linear velocity is 0.982731 m/s and after that it will constant throughout. At 700 rpm the linear velocity is 1.14678 m/s and after that it will constant throughout. At 1000 rpm the linear velocity is 1.638145 m/s and after that it will constant throughout. At 1250 rpm the linear velocity is 2.047681 m/s and after that it will constant throughout. At 1500 rpm the linear velocity is 2.457218 m/s and after that it will constant throughout. At 1750 rpm the linear velocity is 2.86624 m/s and after that it will constant throughout.

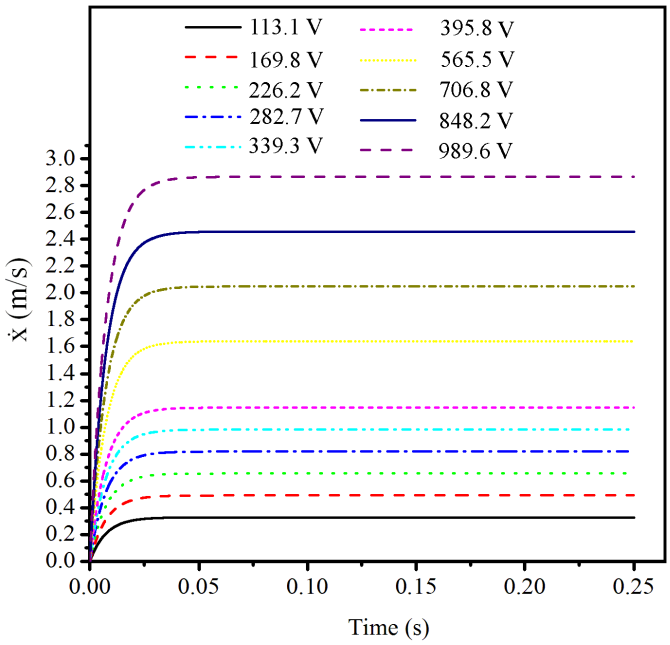

Fig. 3.22 Linear velocity vs. time variation of smaller rotor without eccentricity

In this simulation result the circumferential flow is directly proportional to the journal speed. As the journal speed increases the flow inside the bearing also increases due to which temperature inside the bearing raise and creates a thin film layer.

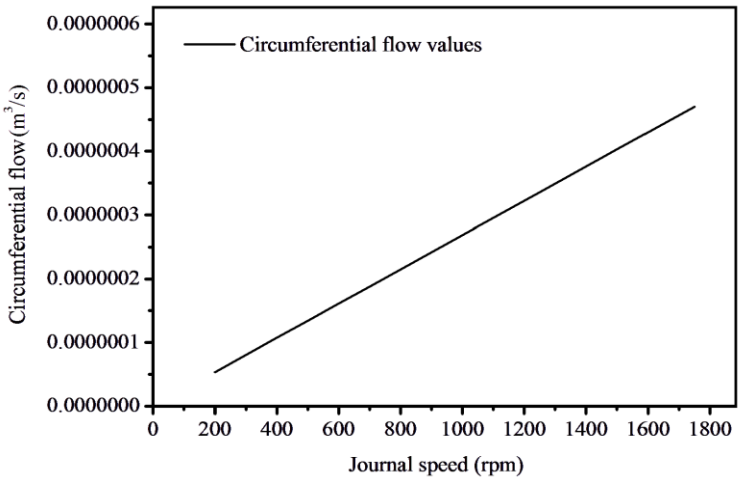

Fig. 3.23 Circumferential flow vs. journal speed variation of smaller rotor without eccentricity

The displacement in x and y direction are shown in Fig. 3.23 when rotor rotates about shaft axis it will displace in x and y direction because of centrifugal force acting outwards. Due to centrifugal force rotor displace from the centroidal axis and gives displacement in x and y direction.

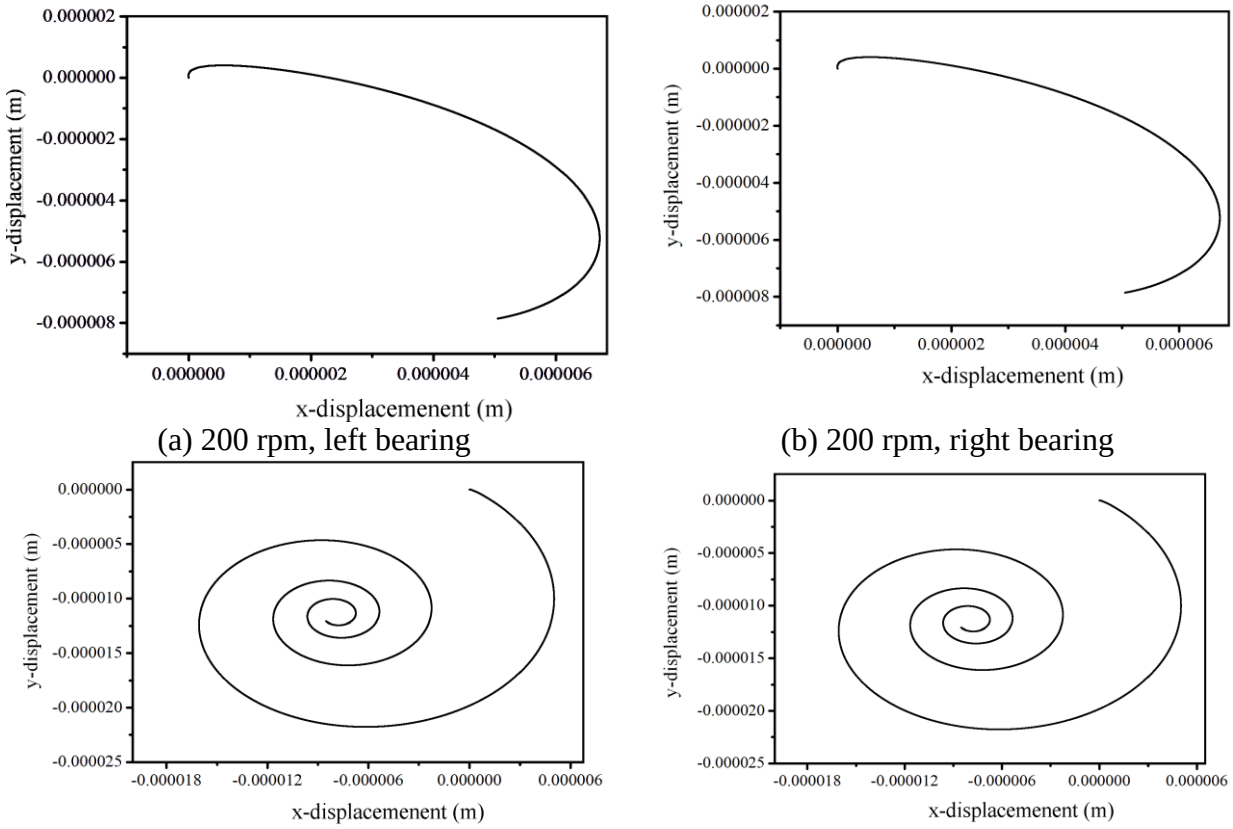

(a) 200 rpm, left bearing

(b) 200 rpm, right bearing

(c) 1750 rpm, left bearing

(d) 1750 rpm, right bearing

Fig. 3.24 Displacements in x and y direction of smaller rotor without eccentricity

3.6.7 *Parameter values of smaller rotor with eccentricity*

The parameter values of smaller rotor with eccentricity as shown in Table 3.8

Table 3.8: Parameter values of smaller rotor with eccentricity

Parameter	Values	Description
K_s	1×10^6 N/m	Stiffness of the shaft
R_s	1×10^2 Ns/m	Damping coefficient of shaft
c	1.1×10^{-4} m	Radial clearance of the bearing
N	200, 300, 400, 500, 600, 700, rpm	Journal speeds
T_i	31.2, 33.2, 35.3, 28.8, 32.4, 35.7 K	Initial temperatures
e	5.016×10^{-6} m	Eccentricity
S_p	1800 J/K	Specific heat of the oil
L	0.0327 m	Bearing Length
ρ	872.5 kg/m^3	Density of the oil
R	0.01575 m	Journal radius
G	9.81 m/s^2	Acceleration due to gravity
m	1.2439 kg	Journal mass
M	0.621 kg	Mass of the disc
J_{xx}	0.1 kgm^2	Rotary inertia in x-direction
J_{yy}	0.1 kgm^2	Rotary inertia in y-direction
J_{zz}	0.2 kgm^2	Rotary inertia in z-direction
L	0.115 m	Distance between left bearing to right bearing
R_r	2 Ns/m	Damping coefficient of motor
μ	5	Constant value
R_m	1 Ns/m	Damping coefficient of motor
V	113.1, 169.65, 226.2, 282.75, 339.3, 395.85, 565.5 V	Voltage
R_e	15 Ns/m	External damping of rotor
R_i	5 Ns/m	Internal damping of rotor
e_1	0.01 m	Rotor eccentricity

K	1×10^6 N/m	Stiffness of the rotor

All parameters values are same except initial temperature (T_i), Voltage (V) and Eccentricity (e) these parameter values are changing according to journal speeds and loads.

3.6.8 *Simulation results of smaller rotor with eccentricity*

Table 3.9: Journal (or motor) angular velocity at different motor speed

Rpm	200	300	400	500	600	700
Rad/s	23.346	29.328	42.58	52.93	60.9836	75.44

In this result the angular velocity of journal or shaft increasing with increase of time. In this result the angular velocity of journal or shaft increasing with increase of time. As the journal rotates at higher motor speed the input voltage also increases with respect to time.

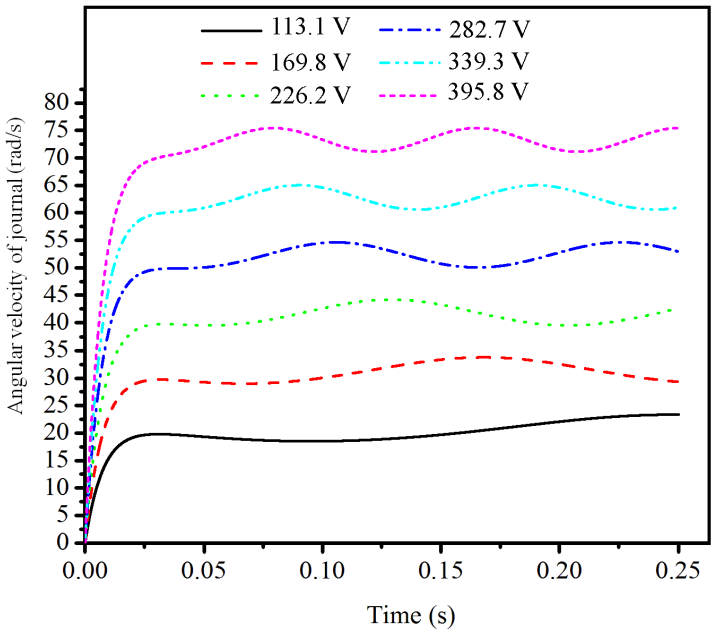

Fig. 3.25 Journal (or motor) angular velocity vs. time at input voltage for smaller rotor with eccentricity

The linear velocity is also increasing with increase of time. At 200 rpm the linear velocity is 0.365141 m/s and after that it will constant throughout. At 300 rpm the linear velocity is 0.458694 m/s and after that it will constant throughout. At 400 rpm the linear velocity is

0.665961 m/s and after that it will constant throughout. At 500 rpm the linear velocity is 0.827861 m/s and after that it will constant throughout. At 600 rpm the linear velocity is 0.953783 m/s and after that it will constant throughout. At 700 rpm the linear velocity is 1.17997 m/s and after that it will constant throughout.

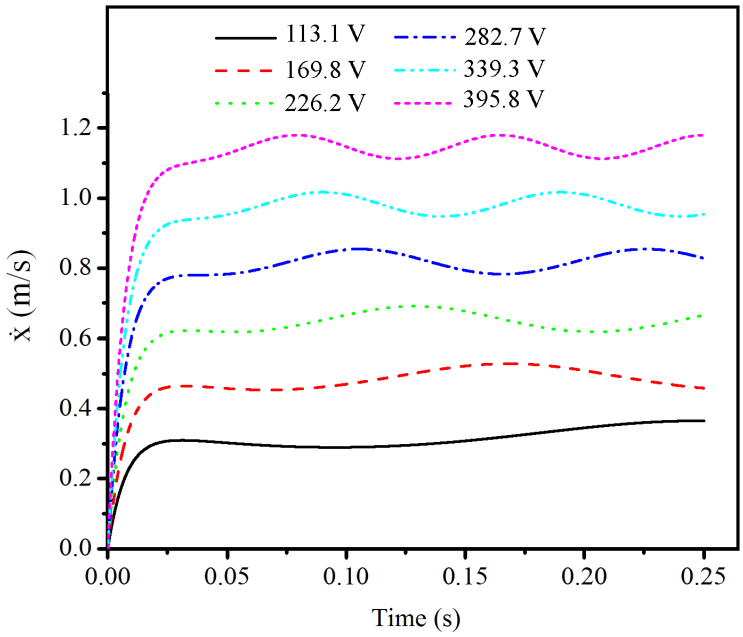

Fig. 3.26 Linear velocity vs. time variation of smaller rotor with eccentricity

In this simulation result the circumferential flow is directly proportional to the journal speed. As the journal speed increases the flow inside the bearing also increases due to which temperature inside the bearing raise and creates a thin film layer.

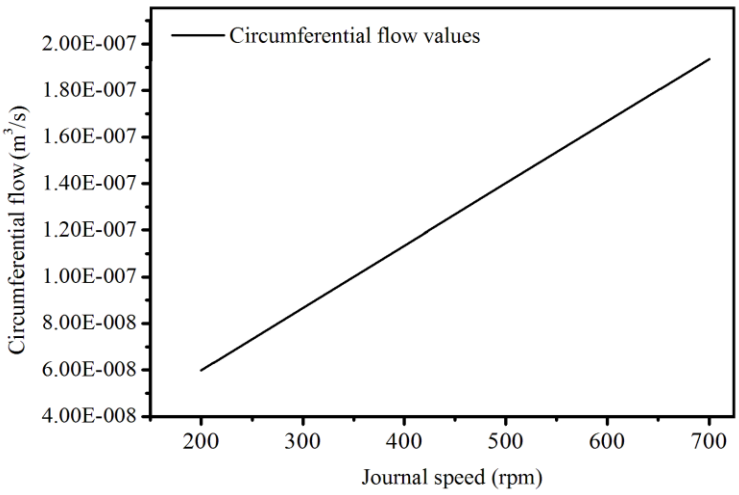

Fig. 3.27 Circumferential flow vs. journal speed variation of smaller rotor with eccentricity

The displacement in x and y direction are shown in Fig. 3.27 when rotor rotates about shaft axis it will displace in x and y direction because of centrifugal force acting outwards. Due to centrifugal force rotor displace from the centroidal axis and gives displacement in x and y direction

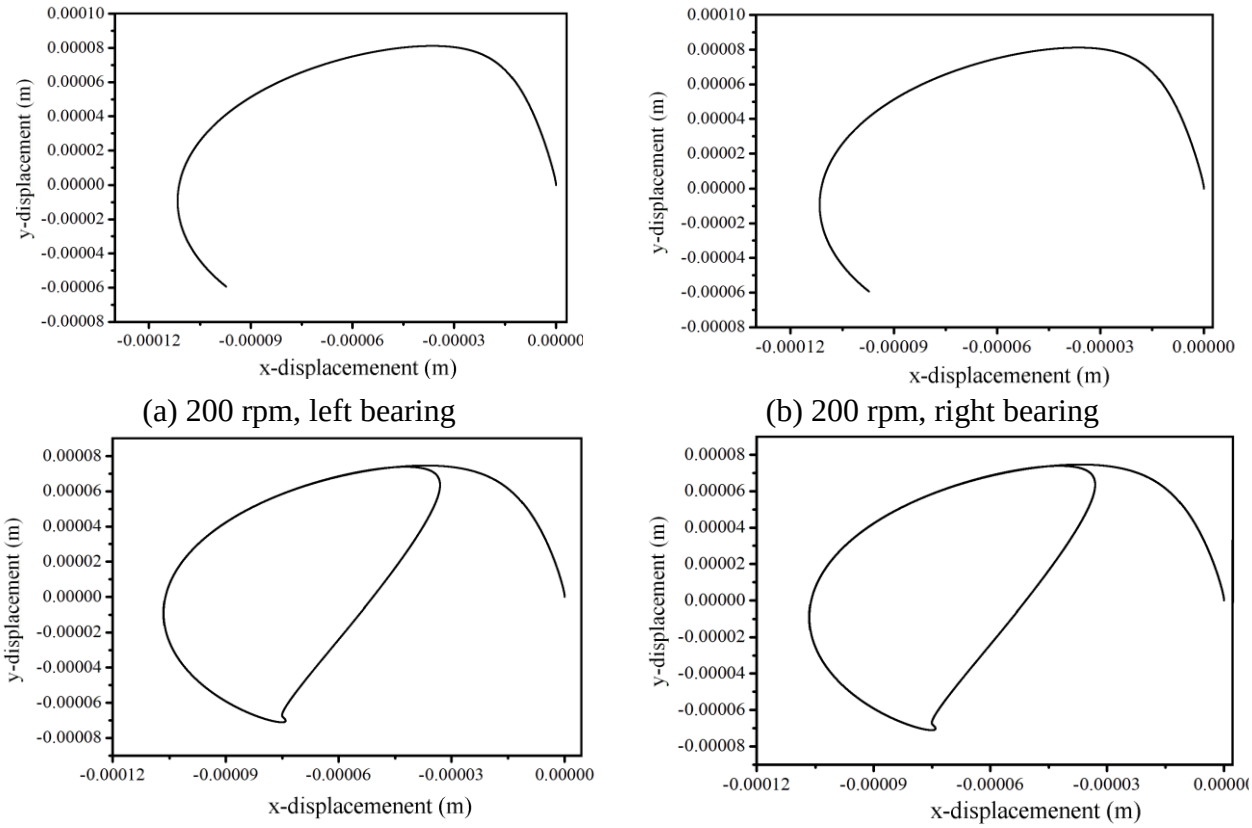

(a) 200 rpm, left bearing (b) 200 rpm, right bearing

(c) 700 rpm, left bearing (d) 700 rpm, right bearing

Fig. 3.28 Displacements in x and y direction of smaller rotor with eccentricity

CHAPTER 4 EXPERIMENTATION ON SHAFT-ROTOR SYSTEM

4.1 Introduction

The experimental work is necessary for validation of simulation results obtained from bond graph model of the shaft-rotor system. The experimental set up consists of base plate, dc motor, stainless steel shaft, journal bearings, motor-shaft coupling. The thermocouples are used for measuring the temperature of the journal oil whose temperature increases due to rotation viscosity of lubricant, speed of the journal and the load carried by the journals. The initial temperature of lubricant is same as atmospheric temperature and flow and temperature of oil change due to different input speeds of the motor and viscosity of lubricant changes due to change of temperature of oil.

4.2 Selection of components and materials

In experimental set up, the assembly of base plate, AISI 304 stainless steel shaft, jaw coupling, motor and bearings is done. Stainless steel shaft has steps on in at both the ends for holding the bearings and rotors on it. The shaft is grounded on its periphery by cylindrical grinding. 100 microns of radial clearance is provided between the journal and the bearing. The pressure of the lubricant increases due to radial clearance, viscosity of oil, rotation of journal. The volume flow rate in the circumferential as well as axial direction changes but the axial flow is negligible. The temperature of lubricant changes due to change of enthalpy of it.

4.2.1 *Bearings*

Bearing as shown in Fig. 4.1 are required to support the loads on the journal particularly when there is relative motion between the components. The bearings used have inner diameter of 31.5 mm and outer diameter of 52.5 mm. Bearings contain split type bush which is made of brass. The brass which is an alloy of copper and zinc is used in bearings and valves due to its low coefficient of friction between the rubbing surfaces. Two split type bushes are hold by bracket which can be adjusted according to the need. Brackets have 2 mm diameter hole through which oil is to be poured continuously in the journal bearing.

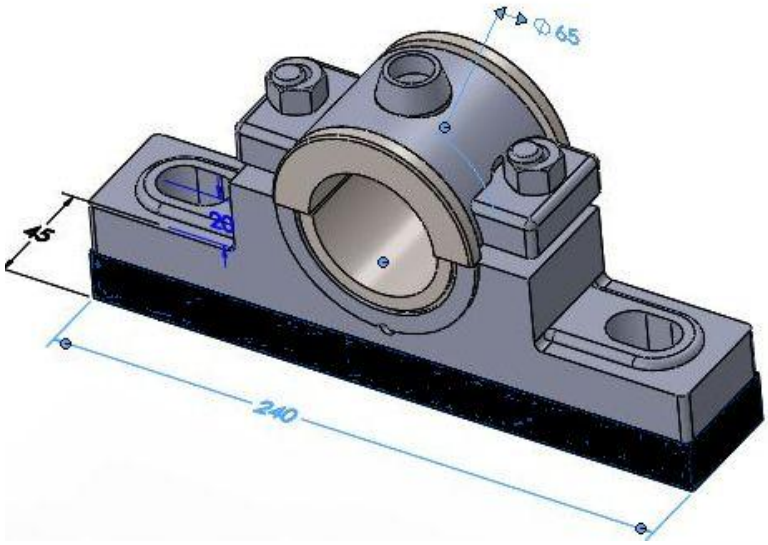

Fig. 4.1 Schema of journal bearing

4.2.2 *Stainless steel shaft*

The shaft is basically used for power transmission in any application. It also carries bending load. The torque given by the motor or prime movers is transmitted through the shaft. The strength of the shaft should be high enough so that the deflection of the shaft under the action of heavy load is minimum. The AISI 304 stainless steel shaft is grounded by cylindrical grinding to provide steps for perfect alignment with coupling. The key way is providing on the surface of shaft at the centre and at the motor end to get tightening of rotor and coupling, respectively. The length of the shaft is of 300.47 mm and the diameter of the shaft on the bearing side is 31.6 mm.

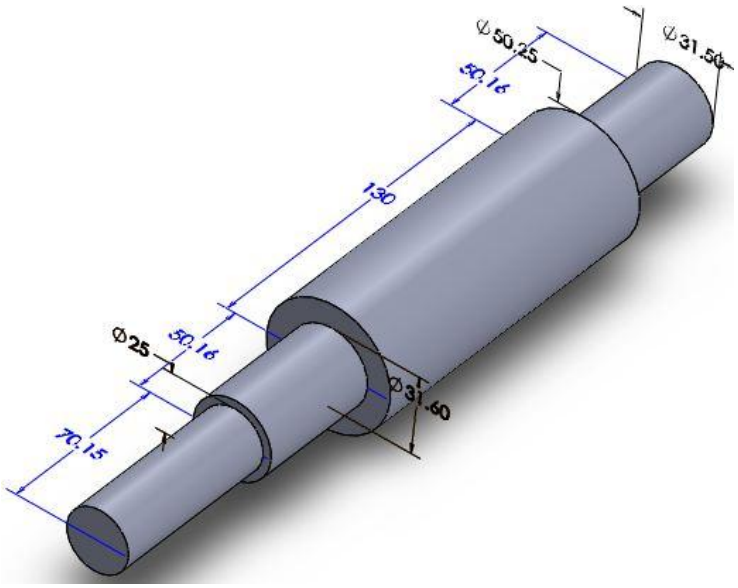

Fig. 4.2 Stainless steel shaft

4.2.3 *Rotor*

Rotors are made up of cast iron (EN8). The rotor either concentric or eccentric is connected with the shaft at the mid position to provide static or dynamic load to the journal bearing as shown in Fig. 4.3 (a)–(d).

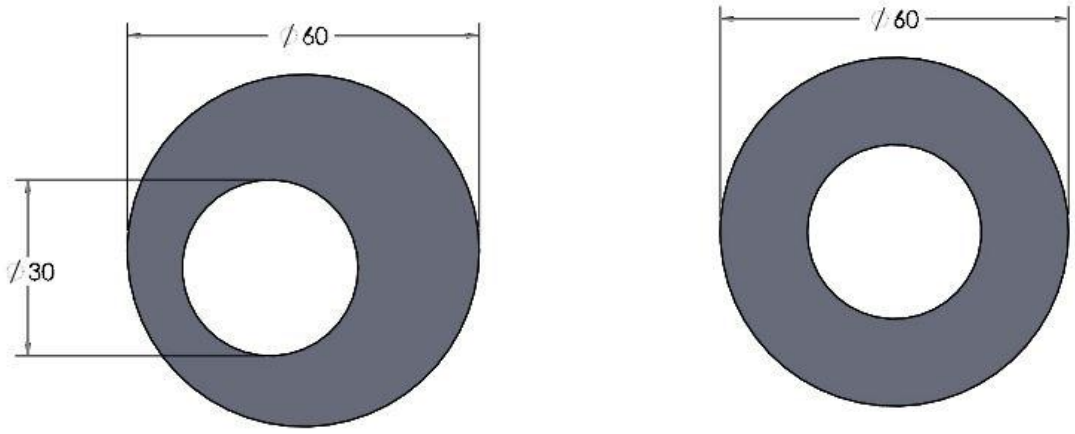

(a) (b)

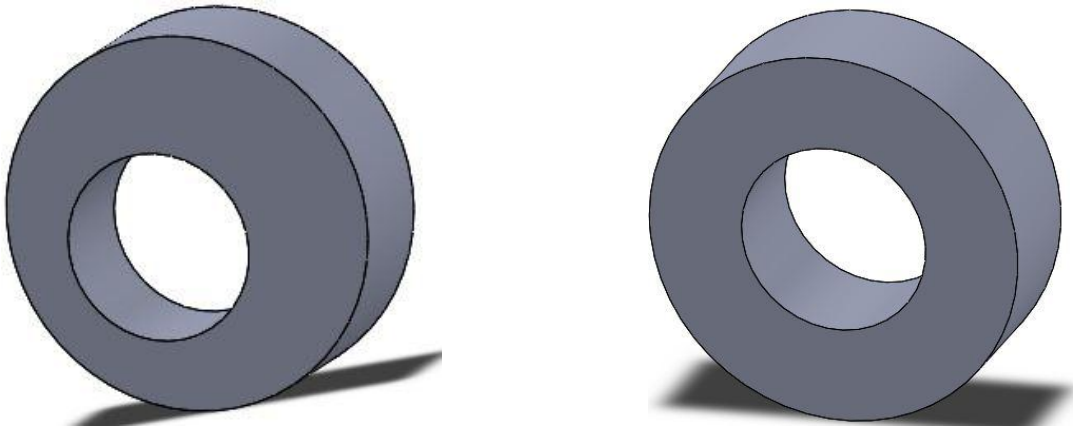

(c) (d)

Fig. 4.3 (a) End view of eccentric rotor, (b) End view of centric rotor, (c) Isometric view of eccentric rotor and (d) Isometric view of centric rotor

The rotors provide the static or dynamic load to the shaft in the running condition. The rotor with eccentricity develops dynamic load on the shaft and as a result of this, fluid film squeezes and more pressure develops. Due to the enhanced pressure or enhanced enthalpy of lubricant, the temperature of it increases. This temperature varies according to pressure developed in fluid film and friction between different layers. The temperature is measured by the k-type thermocouple which is inserted both ends of the bearings through cap-hole and the readings are taken from the digital temperature indicator for different speeds of the shaft. The eccentricity, material and the mass of different rotors are given in Table 4.1. The diameters of smaller and larger rotors are 143.6 mm and 75.9 mm.

Table 4.1: Specifications and material of the rotor

Rotor	Eccentricity (e)	Material	Mass (kg)
Smaller centric	0 mm	Cast iron	0.621
Smaller eccentric	10 mm	Cast iron	0.625
Larger centric	0 mm	EN8	1.274
Larger eccentric	10 mm	EN8	1.301

4.2.4 *Base plate*

The base plate as shown in Fig. 4.4 is used as a rigid support for the experimental set up. Some times vibration occurs during the high speeds of the rotor-shaft, so it is the important to have

rigid base plate. The base plate is rigid enough so that it does not deflect under the action of varying loads. Since the motor, bearings and shaft along with the rotor are mounted on the same plate, the surface flatness is a major concern to avoid any misalignment between shaft and motor-shaft. As the shaft is mounted at a height of 5.08 cm (which is less than the radius of the rotor) from the base plate, a rectangular hole is provided through which rotor can easily rotate without any interference.

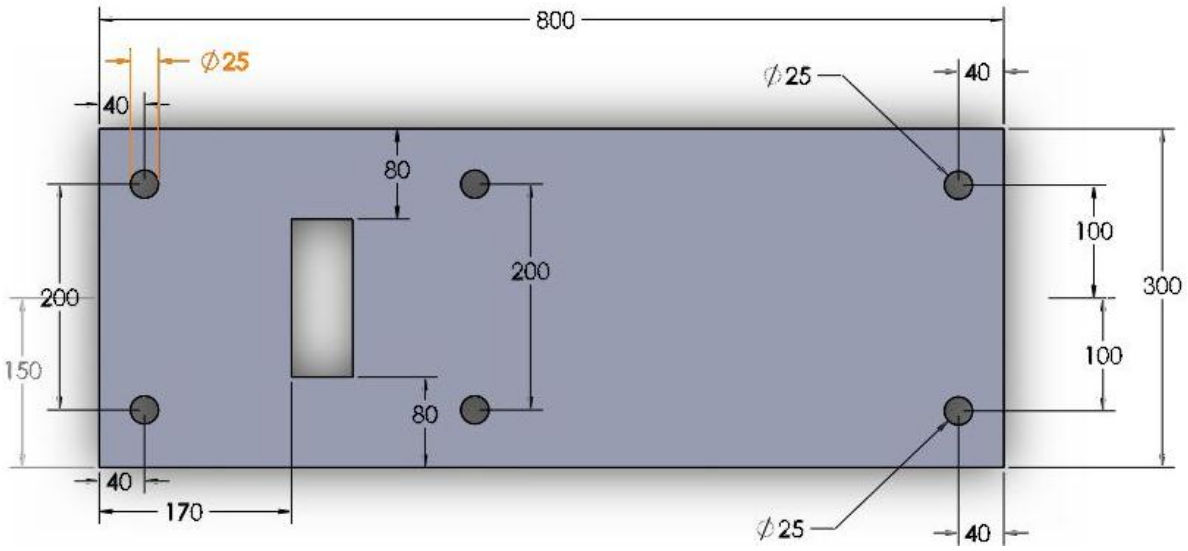

Fig. 4.4 Base plate

4.2.5 *Coupling*

Coupling connects two shafts together to avoid the misalignment problem and provides smooth transmission. The coupling should be flexible enough so that its diameter can be adjusted easily with the shaft and motor. Jaw coupling is used of 60 mm diameter and 100 mm length. The L-keys are provided at both ends of coupling for tight fit. The coupling is shown in Fig. 4.5.

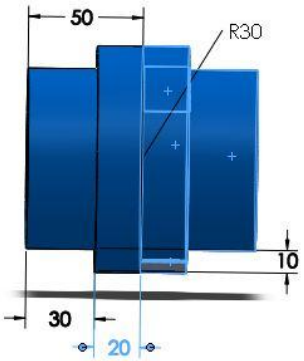

Fig. 4.5 Coupling

4.2.6 *Electric Motor*

Electric motor as shown in Fig. 4.6 is a device which converts electrical energy into the mechanical energy. The motor should have high horse power for proper operation. The motor has 92 W, 8500 rpm, AC/DC type, 1.5 A, 220/230 V.

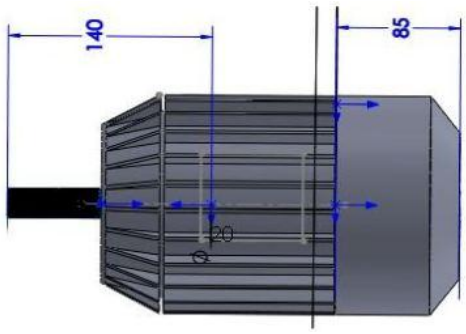

Fig. 4.6 Electric motor

4.2.7 *Thermocouple and digital temperature indicator*

A k-type thermocouple consists of two metal joined together to form two junctions. At one end, the temperature is known and is considered as the reference junction and at the other end, temperature is unknown; this end could be hot or cold and its temperature is to be measured. Thus, the thermocouple measures the unknown temperature of the body with reference to the known temperature. As shown in the Fig. 4.7(a), it consists of two dissimilar wires which are connected to each junction P and Q. The P junction is at a temperature T_1 and Q junction is at temperature T_2. As the two junction are at different temperature, the emf is generated which is a function of temperature. If the temperature of both the junction is same, equal and opposite emf will be generated at both junctions and the net current flowing through the junction is zero. If the two junctions are at different temperatures, the emf will not be equal to zero and there will be a net current flowing through the circuit. The total emf flowing through this circuit depends on the metal used within the circuit as well as the temperature of the two junctions. The device for measuring the current or emf is connected within the circuit of the thermocouple. It measures the amount of emf flowing through the circuit due to the two junctions of the two dissimilar metals maintained at different temperatures. Now, the temperature of the reference junction is already known, while the temperature of the measuring junction is unknown. The output obtained from the thermocouple circuit is calibrated directly against the known temperature. Thus, the voltage

or current output obtained from thermocouple circuit gives the value of unknown temperature directly. Digital temperature indicator shows the value of that temperature as shown in Fig. 4.7(b).

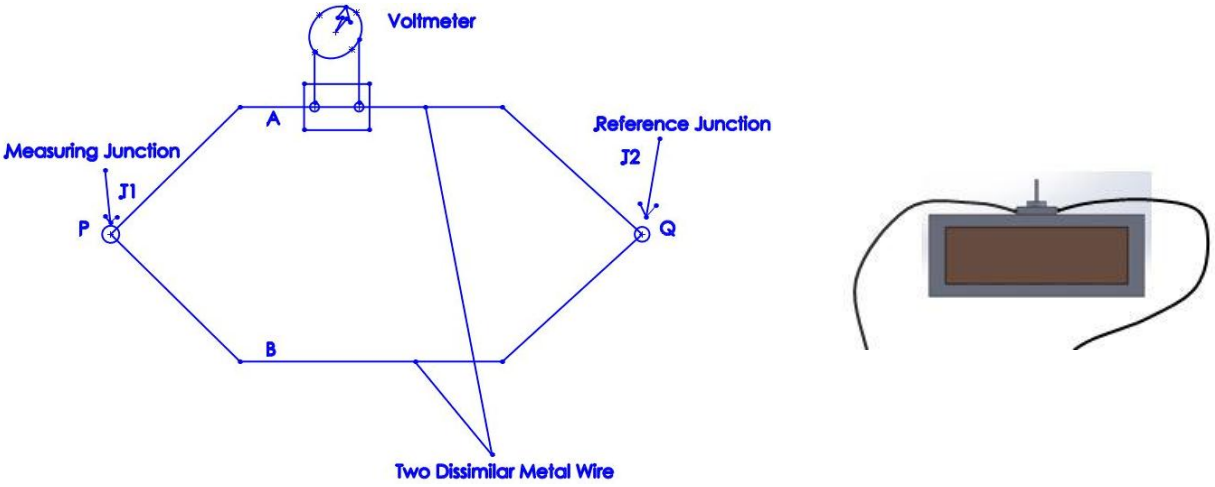

(a) (b)

Fig. 4.7 (a) Thermocouple and (b) Temperature indicator

4.3 System set up

The system set up consisting of base plate, motor, stainless steel shaft, journal bearings, voltage regulator, rotor, coupling, thermocouples and temperature indicator. The set up is prepared for the two type of loading conditions i.e. static and dynamic loading. For achieving this type of condition, the rotors are to be prepared accordingly. Rotors are of two types i.e. centric and eccentric; centric is made for static loads and eccentric is made for dynamic loads. The setup is prepared for the development of temperature inside the journal bearing arrangement. The shaft is placed between two bearings at the ends and motion is transferred to the shaft from the motor through jaw coupling. Thermocouples are inserted at the both ends of the bearing to measure the variation of temperatures at different speeds. Initially, the temperature of lubricant is equal to atmospheric temperature after some time it rises accordingly to the speed and load acting on the shaft by the rotors.

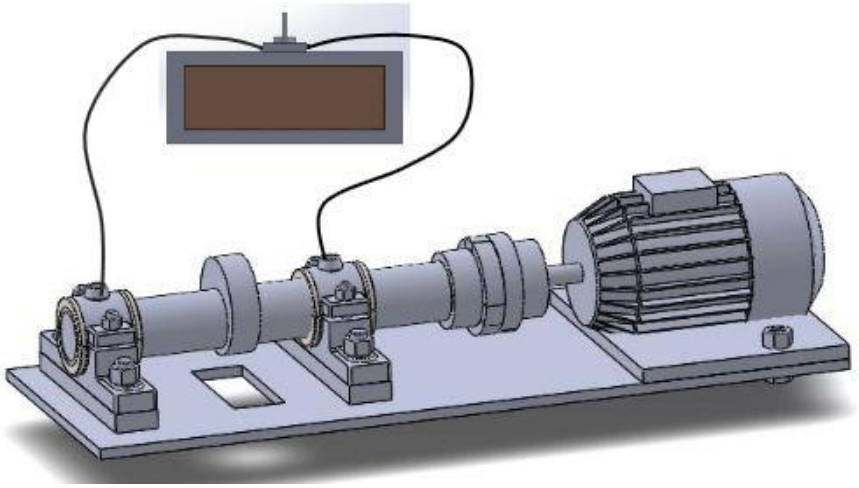

Fig. 4.8 Experimental setup

4.3.1 *Larger rotor with eccentricity*

If the larger rotor with eccentricity is mounted on the shaft, dynamic load acts on the system during rotation of the shaft as shown in the Fig. 4.9. The eccentricity between the mass centre and the geometric centre is 10 mm. The rotor is made of EN8 to avoid distortion or deformation while running at higher speeds. The rotor should be strong enough and have higher stiffness, tensile strength, hardness etc. To remove the irregularities at the outer periphery of the rotor, cylindrical grinding and surface finish operations are done for the rotor.

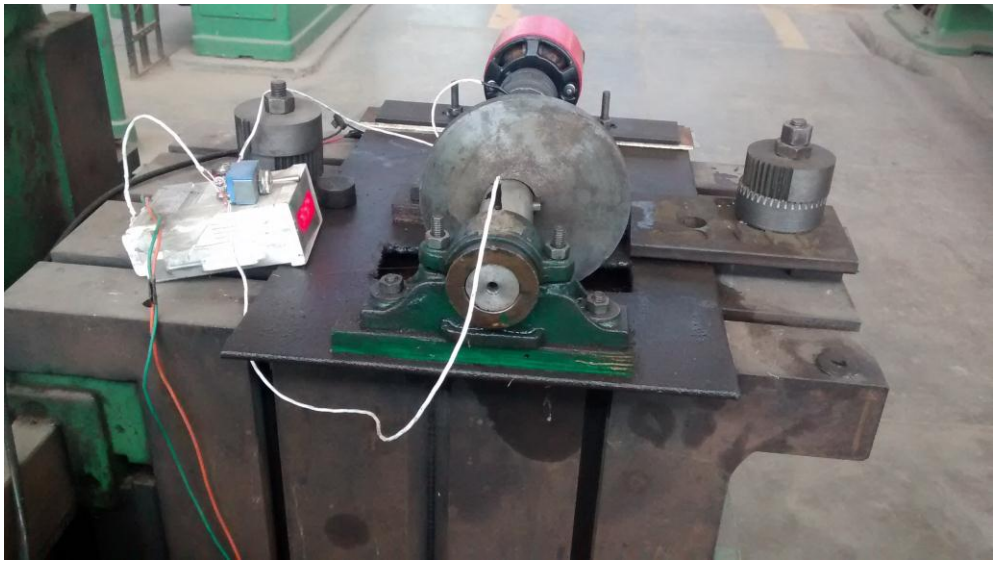

Fig. 4.9 Larger rotor with eccentricity

4.3.2 *Larger rotor without eccentricity*

If the larger rotor with no eccentricity is mounted on the shaft, the load acting on the shaft is static in nature as shown in the Fig. 4.10. The rotor is made of EN8. The cylindrical grinding and surface finish operations are done on the outer circumference of the rotor. The diameter and thickness of the larger rotor are 143.6 mm and 10.6 mm, respectively.

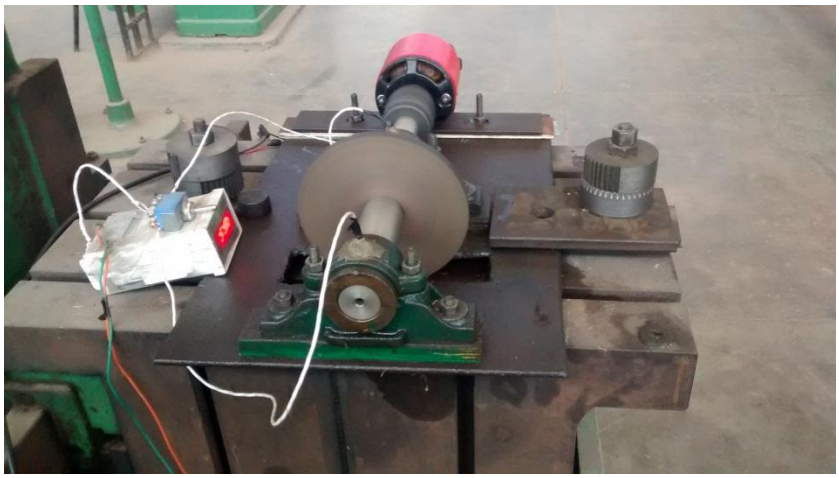

Fig. 4.10 Larger rotor with no eccentricity

4.3.3 *Smaller rotor with eccentricity*

Smaller rotor with eccentricity is mounted on the shaft for giving smaller dynamic loads on the system. The eccentricity between the mass centre and the geometric centre is 10 mm. The rotor is made of cast iron. The cylindrical grinding and surface finish operations are done for the finishing of the circumference of the rotor. The system set up with smaller rotor having eccentricity is shown in the Fig. 4.11. The diameter and the thickness of the rotor are 75.9 mm and 25.8 mm, respectively.

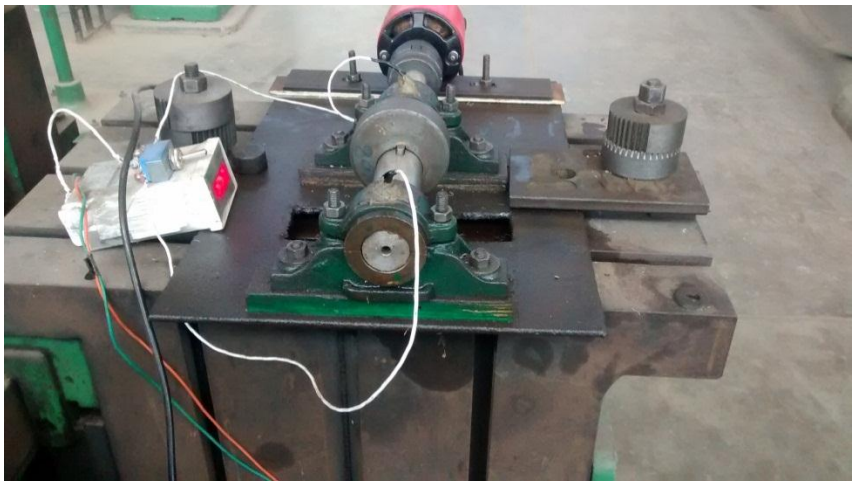

Fig. 4.11 Smaller rotor with eccentricity

4.3.4 *Smaller rotor with no centricity*

If a smaller rotor with no centricity is mounted on the shaft, smaller static load acts on the system. The rotor with no eccentricity is made of cast iron. The diameter and the thickness of the rotor are 75.9 mm and 25.8 mm, respectively. The system set up of smaller rotor without centricity is shown in the Fig. 4.12.

Fig. 4.12 Smaller rotor without centricity

4.4 Experimentation

The experimentation on the setup is performed with two types of rotors i.e. different static and dynamic loads are applied on the shaft having different angular speeds. The speed of the motor can be changed by means of voltage regulator and the speed is measured by tachometer. The initial viscosity of oil (SAE40) is approximately 0.0014 Ns/m^2 and the lubricant is poured into the bearings and the initial temperature of oil is also noted at the bearings ends; then after every five minutes of time interval variation of temperature is noted down. The temperature of oil increases gradually and after some time, the temperature reaches to a steady state condition. The variation of temperature is measured by thermocouple which is connected to the temperature indicator. The experimentation is done by four different rotors and all of the rotors run at different speeds.

4.4.1 *Experimentation by larger rotor without eccentricity*

The larger rotor without eccentricity is coupled with the shaft to provide static load to the shaft. The larger rotor is coupled to the shaft by means of key-way at the mid-point of the bearings. Bearing are adjusted by the bracket according to the journal diameter; oil is poured through the oil hole. As oil enters into the clearance between journal and bearing, a film of oil is produced when journal starts rotating. The initial motor speed and temperature are 200 rpm and 22.7℃, respectively. This temperature increases with time. After 20 minutes of experimentation this temperature rises to a steady state temperature of 24.9℃. In another experiment, the initial speed of rotor and the temperature of lubricant are 300 rpm and 31.6℃, respectively. After 35 minutes, temperature of lubricant rises upto steady state temperature of 35.9℃. The similar experimentation is performed on the other journal speeds and the variations of temperatures are measured. The experimental results of larger rotor without eccentricity are given in Table 4.2 and Fig 4.13.

Table 4.2: Temperature of oil at different speeds for larger rotor without eccentricity

Journal speed (rpm)	Initial temperature (℃)	Steady-state temperature (℃)	Increase of temperature(℃)
200	22.7	24.9	2.2
300	31.6	35.9	4.3

400	25.6	30.2	4.6
500	24.6	29.8	5.2
600	28.6	34.3	5.7
700	25.2	32.6	7.4
800	29.4	37.3	7.9
900	27.2	36.8	9.6
1000	28.8	40.5	11.7

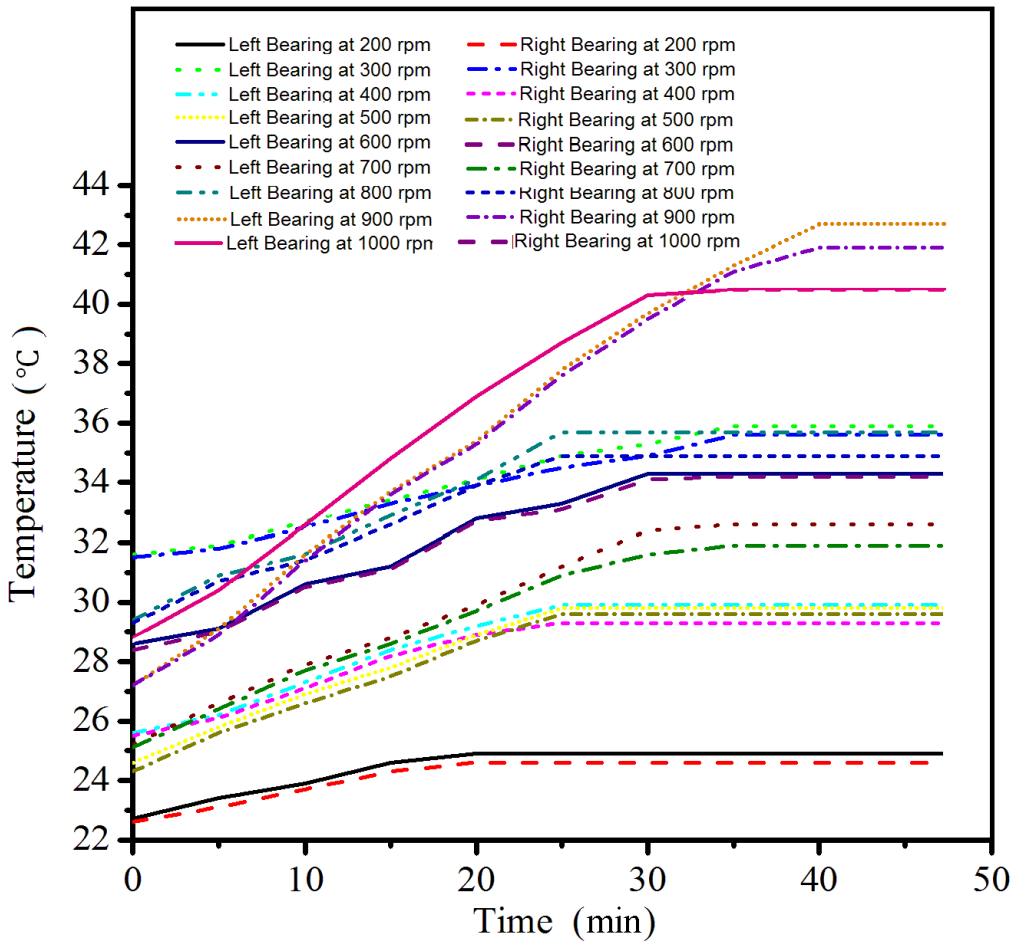

Fig. 4.13 Variations of temperature of lubricant with time for different speeds of larger rotor without eccentricity

4.4.2 *Larger rotor with eccentricity*

The larger rotor with eccentricity is mounted on the shaft to provide dynamic loads to the system. The shaft-rotor system is built up on the two journal bearings and oil is poured by simple manual lubrication system. The initial temperature of lubricant and speed of the journal are 25℃ and 200 rpm, respectively. After 20 minutes, the temperature rises to steady state temperature of 27.2℃. Here, temperature of oil due to dynamic loading rises faster as compared to static loading. As the temperature of oil increases, the viscosity of it decreases gradually. In the second experiment, initial temperature and journal speed are 25.1℃ and 300 rpm, respectively. After 30 minutes, this temperature reaches steady state temperature of 29.9℃. The similar experimentation is performed with the same rotor but at the different rotor speeds. The experimental results of the larger rotor with eccentricity are shown in Table 4.3 and Fig 4.14.

Table 4.3: Temperature of oil at different speeds for larger rotor with eccentricity

Journal speed (rpm)	Initial temperature (℃)	Final temperature (℃)	Increase of temperature(℃)
200	25	27.2	2.2
300	25.1	29.9	4.8
400	35.3	42.1	6.8
500	31.4	40.3	8.9
600	32.4	42.9	10.5

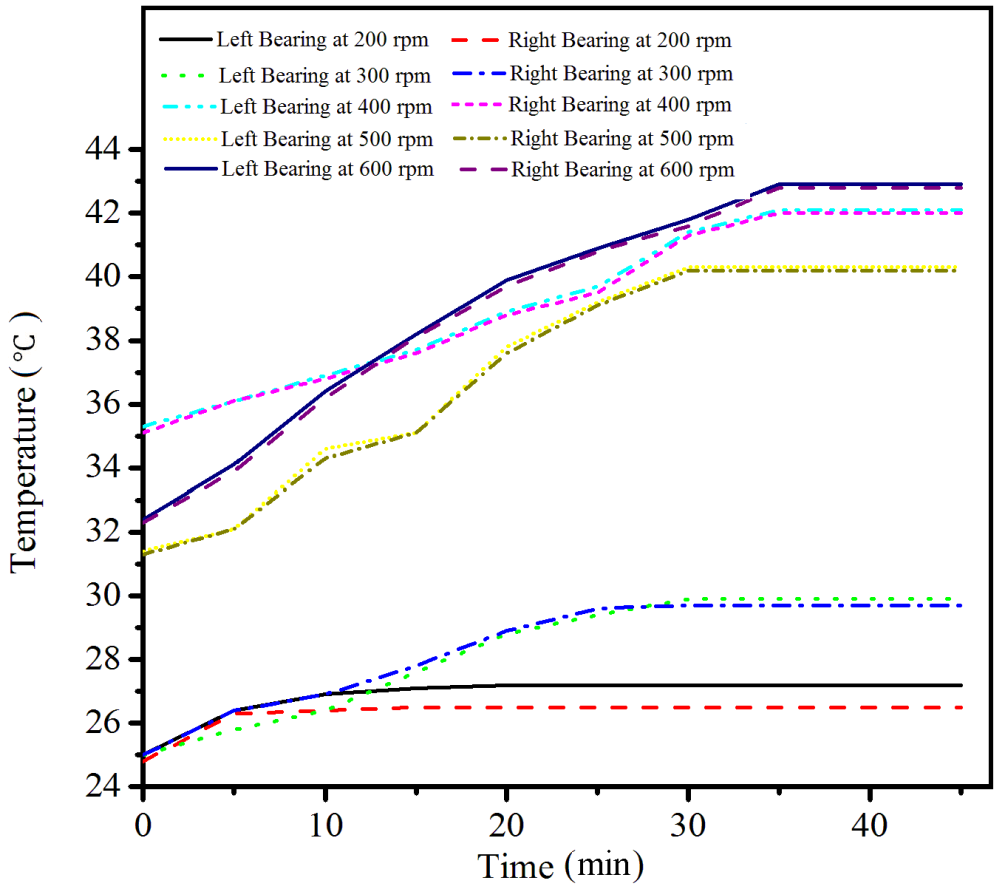

Fig. 4.14 Variations of temperature of lubricant with time for different speeds of larger rotor with eccentricity

4.4.3 *Smaller rotor without eccentricity*

The smaller rotor without eccentricity is mounted on the shaft to provide lesser static load to the shaft. The smaller rotor is attached to the shaft between both the journal-bearings by means of key-way. Bearings are adjusted by the bracket according to the journal diameter and oil is poured through the oil-hole. As oil enters into the clearance between journal and bearing, pressure is developed when journal starts rotating. Initially, the speed of the journal and the temperature of lubricant are 200 rpm and 27.4℃, respectively. After 20 minutes of experimentation, the temperature of oil rises to a steady state value of 29.4℃. Another experimentation is performed when the speed of the shaft and temperature of oil are 300 rpm and 23.4℃, respectively. After 30 minutes, temperature of oil rises up to 25.7℃ to reach to a steady state value. Similar experimentations are performed with different shaft speeds. The experimental results of smaller rotor without eccentricity are given in Table 4.4 and Fig 4.15.

Table 4.4: Temperature of oil at different speeds for smaller rotor without eccentricity

Journal speed (rpm)	Initial temperature (℃)	Final temperature (℃)	Increase of temperature(℃)
200	27.4	29.4	2
300	23.4	25.7	2.3
400	27.7	30.5	2.8
500	27.6	30.8	3.2
600	34.3	39.1	4.8
700	33.6	39.8	6.2
1000	35.4	45.2	9.8
1250	29.5	39.7	10.2
1500	23	40.4	17.4
1750	24.2	43.9	19.7

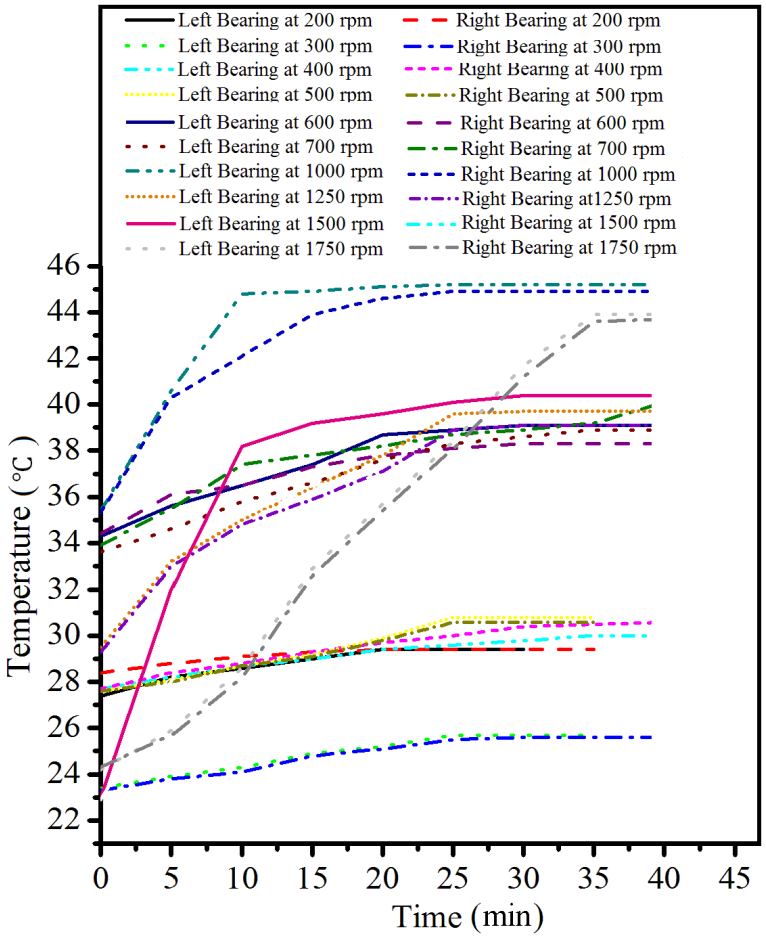

Fig. 4.15 Temperature of oil vs. time at different speeds for smaller rotor without eccentricity

4.4.4 *Smaller rotor with eccentricity*

The smaller rotor with eccentric is attached to the shaft to provide dynamic loads to the system. The smaller rotor is placed between two bearings and oil is poured by simple manual lubrication system. The initial temperature of oil and journal speed are 31.2℃ and 200 rpm, respectively. After 25 minutes, the temperature rises to a steady state temperature of 33.9℃. Here, temperature rises faster than the system having rotor without eccentricity as dynamic load is applied in the earlier case; viscosity of the oil or lubricant decreases with the increase of temperature. In another experiment, the initial temperature of oil and shaft speed are 33.2℃ and 300 rpm, respectively. After 25 minutes, the temperature of lubricant rises to a steady state temperature of 37.4℃. The similar experimentations are performed by other rotors with different speeds. The experimental results of smaller rotor with eccentricity are given in Table 4.5 and Fig 4.16.

Table 4.5: Temperature variations with different shaft speeds for smaller rotor with eccentricity

Journal speed (rpm)	Initial temperature (℃)	Final temperature (℃)	Increase of temperature(℃)
200	31.2	33.9	2.7
300	33.2	37.4	4.2
400	35.3	41.4	6.1
500	28.8	36.2	7.4
600	32.4	40.9	8.5
700	35.7	44.9	9.2

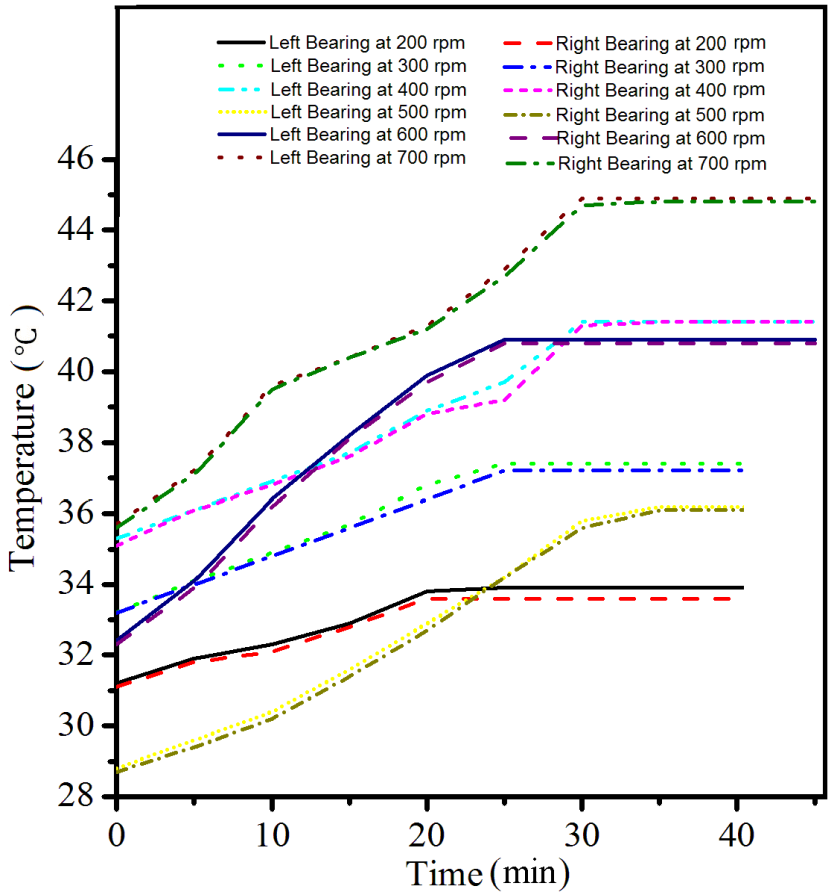

Fig. 4.16 Variation of temperature with time at different speeds of smaller rotor with eccentricity

4.5 Validation of results

The results obtained by the experiment are further validated by means of the simulation results of the same system. Bond graph modelling technique is used for modelling the rotor shaft system along with journal bearings. The results obtained by the bond graph and by the experiment are nearly same.

4.5.1 *Comparison between simulation and experimental results for larger rotor with eccentricity*

The steady-state temperature of lubricant of journal bearing upon which shaft-larger rotor with eccentricity are mounted is compared between experiment and simulation. The steady-state temperatures are close to each other. The results obtained by the experiment and bond graph modelling are shown in Table 4.6 and Fig 4.17.

Table 4.6: Simulation and experimental results for larger rotor with eccentricity

Sl. no.	Journal speed (rpm)	Experimental steady-state temperature (°C)	Simulation steady-state temperature (°C)
1	200	27.2	29.19
2	300	29.9	30.65
3	400	42.1	40.22
4	500	40.3	38.03
5	600	42.9	39.77

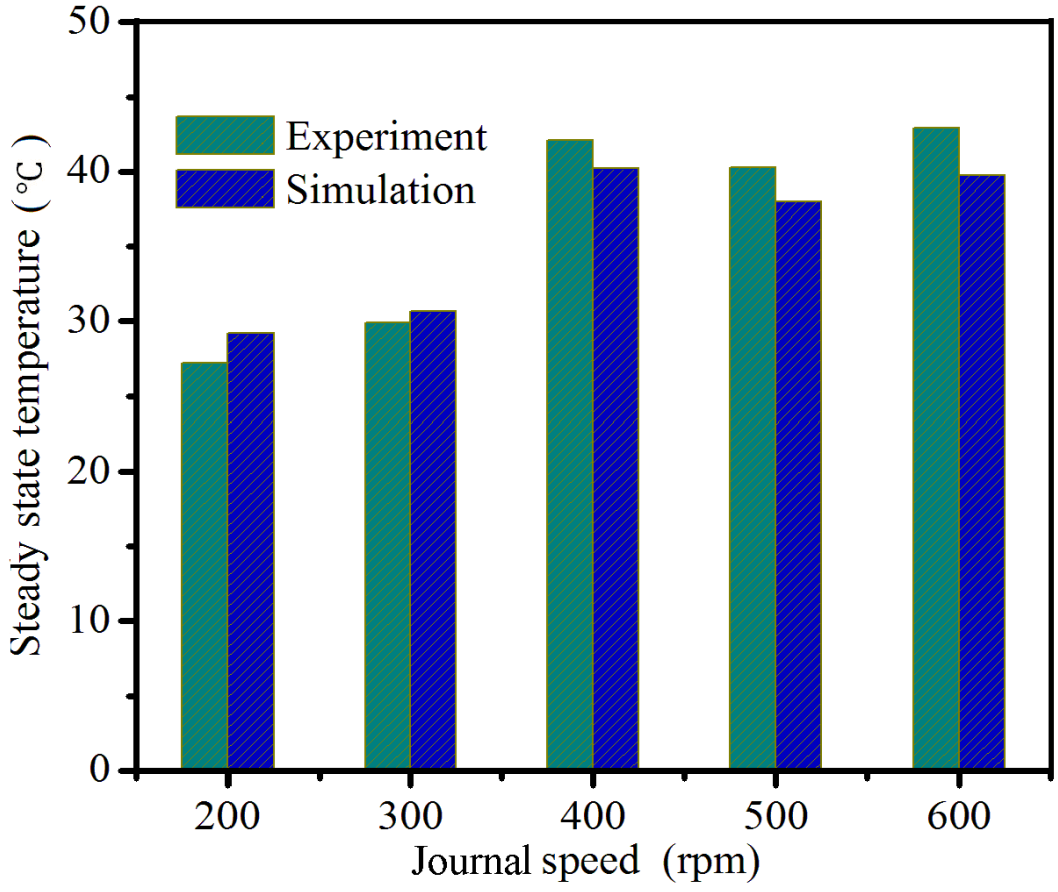

Fig. 4.17 Simulation vs. experimental temperature for larger rotor with eccentricity

4.5.2 *Simulation and experimental results for larger rotor without eccentricity*

The steady-state temperature of lubricant of journal bearing upon which shaft-larger rotor without eccentricity are mounted is compared between experiment and simulation. The steady-state temperatures are close to each other. The results obtained by the experiment and bond graph modelling are shown in Table 4.7 and Fig 4.18.

Table 4.7: Simulation and experimental results for larger rotor without eccentricity

Sl. no.	Journal speed (rpm)	Experimental steady-state temperature (℃)	Simulation steady-state temperature (℃)
1	200	24.9	29.92
2	300	35.9	35.69
3	400	29.9	32.14
4	500	29.8	32.60
5	600	34.3	36.66
6	700	32.6	35.13
7	800	35.7	39.13
8	900	42.7	38.45
9	1000	40.5	40.32

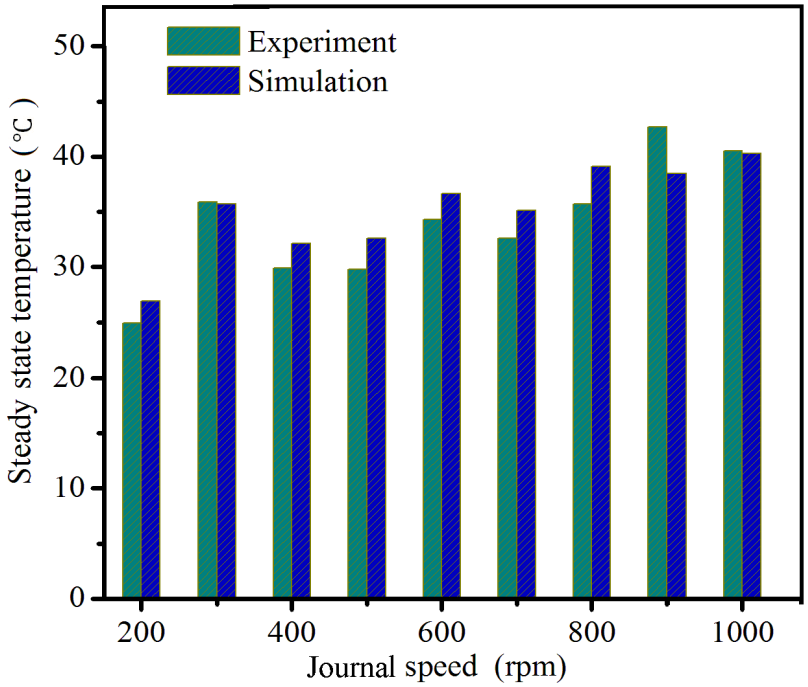

Fig. 4.18 Simulation vs. experimental temperature for larger rotor without eccentricity

4.5.3 *Comparison between simulation and experimental results for smaller rotor with eccentricity*

The steady-state temperature of lubricant of journal bearing upon which shaft-larger rotor with eccentricity are mounted is compared between experiment and simulation. The steady-state temperatures are close to each other. The results obtained by the experiment and bond graph modelling are shown in Table 4.8 and Fig 4.19.

Table 4.8: Simulation and experimental results for smaller rotor with eccentricity

Sl. no.	Journal speed (rpm)	Experimental steady-state temperature (℃)	Simulation steady-state temperature (℃)
1	200	33.9	34.39
2	300	37.4	37.41
3	400	41.4	40.22
4	500	36.2	36.01
5	600	40.9	39.77
6	700	44.9	43.12

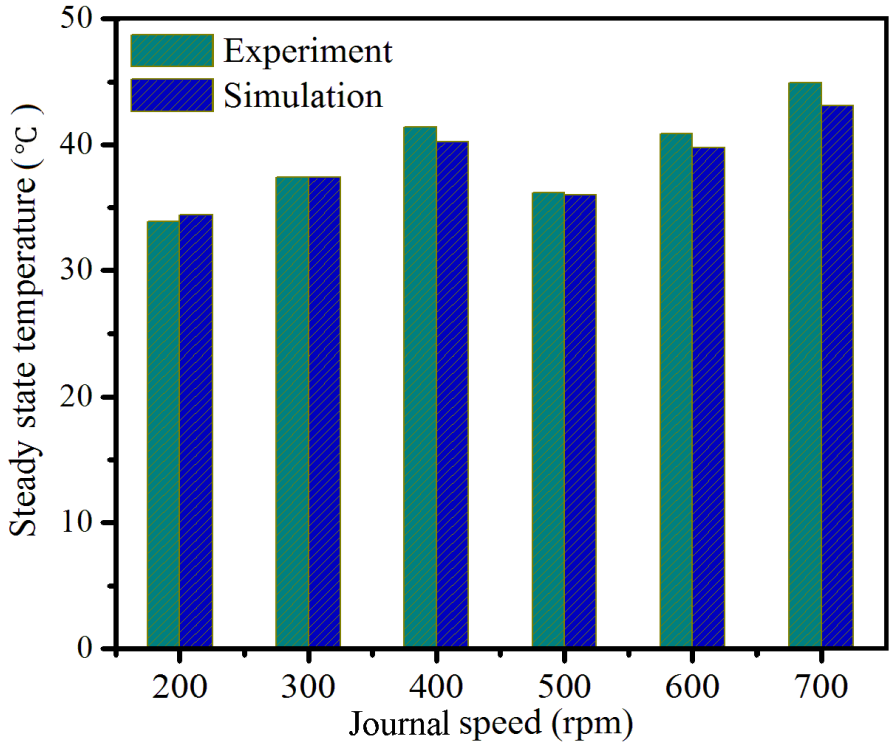

Fig. 4.19 Simulation vs. experimental temperature for smaller rotor with eccentricity

4.5.4 *Comparison between simulation and experimental results for smaller rotor without eccentricity*

The steady-state temperature of lubricant of journal bearing upon which shaft-larger rotor without eccentricity are mounted is compared between experiment and simulation. The steady-state temperatures are close to each other. The results obtained by the experiment and bond graph modelling are shown in Table 4.9 and Fig 4.20.

Table 4.9: Simulation and experimental results for smaller rotor without eccentricity

Sl. no.	Journal speed (rpm)	Experimental steady-state temperature (℃)	Simulation steady-state temperature (℃)
1	200	29.4	30.87
2	300	25.7	29.07
3	400	30	33.78
4	500	30.8	34.85
5	600	39.1	41.06
6	700	39.8	41.39
7	1000	45.2	45.01
8	1250	39.7	52.68
9	1500	40.4	40.14
10	1750	43.9	42.31

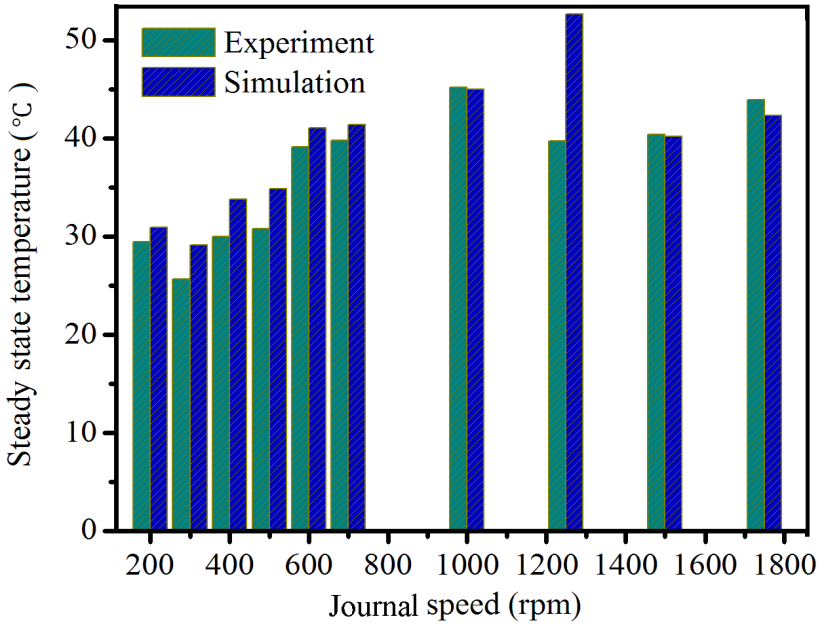

Fig. 4.20 Simulation vs. experimental temperature for smaller rotor without eccentricity

CHAPTER 5 CONCLUSIONS AND SCOPE FOR FUTURE WORK

5.1 Conclusions

The main objective of this thesis work is determine the temperature of the oil inside the journal bearing arrangement under varying loads at different journal speeds. To achieve this, an indigenous experimental setup is fabricated to measure lubricant temperature rise and validate the results with those obtained from bond graph simulation. Experiments are performed at different journal speeds with varying loads to measure temperature rise experimentally. Based on the results obtained from experimental, simulation and their comparison the following conclusions are drawn.

- As voltage increases angular velocity also increases. At 0.025 s the angular velocity is achieve steady state condition in larger rotor without eccentricity. The steady state condition for other rotors is different.
- Linear velocity also increases as voltage increases and at 0.3 m/s the linear velocity of rotor is constant throughout in larger rotor without eccentricity. The steady state condition is different for other rotors.
- Circumferential flow and journal speeds have almost linear relationship in all rotors.
- The minimum and maximum rotation of rotor shows it going to be stabilize in very short time. The graph shows the same nature of left and right end bearings.
- The rise in temperature is 2℃ at 200 rpm to 12℃ at 1000rpm in larger rotor without eccentricity.
- Similarly, rise in temperature is 2.2℃at 200 rpm to 10.5℃ approx. at 600 rpm in larger rotor with eccentricity.
- In smaller rotor without eccentricity the rise in temperature is 2℃ at 200 rpm to 19.5℃ approx. at 1750 rpm.
- The rise in temperature is 2.7℃ at 200 rpm to 9.2℃ approx. at 700 rpm in smaller rotor with eccentricity.

5.2 Scope of future work

Future work may be carried out in the following areas.

- Pressure variation can be predicted and validated for finite journal bearing.
- Variation in temperature rise can be predicted and validated considering the surface roughness, surface conditions of the bearing.
- The study may carried out for different grades of oils.
- It may carried for changing clearance ratio, length to diameter ratio.

REFRENCES

[1] Smalley, A. J., and H. McCallion. Paper 5: The Effect of Journal Misalignment on the Performance of a Journal Bearing under Steady Running Conditions. In: *Proceedings of the Institution of Mechanical Engineers, Conference Proceedings*, 1966 vol. 181, pp. 2: 45-54. SAGE Publications.

[2] Patir, Nadir, and H. S. Cheng. An average flow model for determining effects of three-dimensional roughness on partial hydrodynamic lubrication. *Journal of Tribology* 100, 1978, 1: 12-17.

[3] Hamrock, Bernard J., and Duncan Dowson. Isothermal elastohydrodynamic lubrication of point contacts: Part 1—Theoretical formulation. *Journal of Tribology*, 1976, 2: 223-228.

[4] Booker, J. F. Dynamically loaded journal bearings: mobility method of solution. *Journal of Fluids Engineering*, 1965, 3:537-546.

[5] Paranjpe, Rohit S., and Taeyoung Han. A study of the thermohydrodynamic performance of steadily loaded journal bearings. *Tribology transactions* 1994, 4: 679-690.

[6] Tripathi, K., S. Rajput, and S. Gadakh. Effect of Various Bearing Design Parameters on the Operating Temperature of Hydrodynamic Journal Bearing. *IUP Journal of Mechanical Engineering*, 2013.

[7] Gu, Lili, and Fulei Chu. "An analytical study of rotor dynamics coupled with thermal effect for a continuous rotor shaft." *Journal of Sound and Vibration* 333, 2014, 17: 4030-4050.

[8] Yoon, Se Young, Zongli Lin, and Paul E. Allaire. "Introduction to Rotor Dynamics." In *Control of Surge in Centrifugal Compressors by Active Magnetic Bearings*, pp. 17-55. Springer London, 2013.

[9] Payyoor, Narayanan, Mayank Tiwari, and Kshitij Gupta. "Non-Linear Dynamics, Instability and Chaos of Two Spool Aero Gas Turbine Rotor System." In *ASME 2013 Gas Turbine India Conference*, pp. V001T05A006-V001T05A006. American Society of Mechanical Engineers, 2013.

[10] Özşahin, O., H. N. Özgüven, and E. Budak. "Analytical modeling of asymmetric multi-segment rotor–bearing systems with Timoshenko beam model including gyroscopic moments." *Computers & Structures* 144 (2014): 119-126.

[11] Lacarbonara, Walter, Hadi Arvin, and Firooz Bakhtiari-Nejad. "A geometrically exact approach to the overall dynamics of elastic rotating blades—part 1: linear modal properties." *Nonlinear Dynamics* 70, no. 1 (2012): 659-675.

[12] A Pandya, D. H., S. H. Upadhyay, and S. P. Harsha. "Nonlinear Dynamic Behavior of Balanced Rotor Bearing System Due to Various Localized Defects." In *Proceedings of International Conference on Advances in Tribology and Engineering Systems*, pp. 345-357. Springer India, 2014.

[13] Jinchang, Lu, and Wang Yi. "Vibration Analysis of Multi-Shaft Rotor System with Coupled Gear Mesh." *Journal of Mechanical Transmission* 9 (2013): 033.

[14] Gu, Lili, and Fulei Chu. "An analytical study of rotor dynamics coupled with thermal effect for a continuous rotor shaft." *Journal of Sound and Vibration* 333, no. 17 (2014): 4030-4050.

[15] Lijesh, K. P., Harish Hirani, and P. Samanta. "Theoretical and Experimental Study for Hybrid Journal Bearing." *International Journal of Scientific & Engineering Research* 6, no. 2 (2015): 133-139.

[16] Gertzos, K. P., P. G. Nikolakopoulos, A. C. Chasalevris, and C. A. Papadopoulos. "Wear identification in rotor-bearing systems by measurements of dynamic bearing characteristics." *Computers & structures* 89, no. 1 (2011): 55-66.

[17] Bompos, Dimitrios A., and Pantelis G. Nikolakopoulos. "Rotordynamic analysis of a shaft using magnetorheological and nanomagnetorheological fluid journal bearings." *Tribology Transactions* just-accepted (2015): 10-17.

[18] Kango, S., R. K. Sharma, and R. K. Pandey. "Thermal analysis of microtextured journal bearing using non-Newtonian rheology of lubricant and JFO boundary conditions." *Tribology International* 69 (2014): 19-29.

[19] Baskar, S., and G. Sriram. "Experimental analysis of hydrodynamic journal bearing under different biolubricants." In *Advances in Engineering, Science and Management (ICAESM), 2012 International Conference on*, pp. 132-135. IEEE, 2012.

[20] Sekii, Yoichi, Hiroshi Konno, and Chiharu Fujii. "Hydrodynamic bearing apparatus and spindle motor and disk drive apparatus including the same." U.S. Patent 8,724,257, issued May 13, 2014.

[21] Papadopoulos, C. I., L. Kaiktsis, and M. Fillon. "Computational fluid dynamics thermohydrodynamic analysis of three-dimensional sector-pad thrust bearings with rectangular dimples." *Journal of Tribology* 136, no. 1 (2014): 011702.

[22] Muzakkir, S. M., K. P. Lijesh, and Harish Hirani. "Tribological failure analysis of a heavily-loaded slow speed hybrid journal bearing." *Engineering Failure Analysis* 40 (2014): 97-113.

[23] Nakhaeinejad, Mohsen, and Michael D. Bryant. "Dynamic modeling of rolling element bearings with surface contact defects using bond graphs." *Journal of Tribology* 133, no. 1 (2011): 011102.

[24] Nakhaeinejad, Mohsen, and Michael D. Bryant. "Dynamic modeling of rolling element bearings with surface contact defects using bond graphs." *Journal of Tribology* 133, no. 1 (2011): 011102.

[25] Li, Zhihua, Hongguang Yang, and Jun Yu. "Modelling and optimisation of PMSM-precision reducer system with Modelica." *International Journal of Materials and Structural Integrity* 6, no. 2-4 (2012): 319-330.

[26] Merzouki, Rochdi, Arun Kumar Samantaray, Pushparaj Mani Pathak, and Belkacem Ould Bouamama. "Rigid body, flexible body, and micro electromechanical systems." In *Intelligent Mechatronic Systems*, pp. 281-433. Springer London, 2013.

[27] Mukherjee A, Karmakar R, and Samantaray AK. *Bond Graph in Modelling, Simulation and fault Identification*. FL: CRC Press, 2006.

[28] Majumdar, B. C. *Introduction to tribology of bearings*. S. Chand Limited, 2008,p.38.

[29] Bhattacharyya, R., Mukherjee, A. and Samantaray, A.K. Harmonic oscillations of non-conservative, asymmetric, two-degree-of-freedom systems. *J. Sound and Vib.*, 2004, **264**, 973-980.

[30] Mane, Ravindra M., and Sandeep Soni. "Analysis of Hydrodynamic Plain Journal Bearing." In *Excerpt from the Proceedings of the 2013 COMSOL Conference in Bangalore*.

[31] Mukherjee A, Karmakar R, and Samantaray AK. *Bond Graph in Modelling, Simulation and fault Identification*. FL: CRC Press, 2006, pg.270.

CURRICULUM VITAE

Shubham Choudhary did his graduation from SDCET, Ghaziabad in Bachelor of Technology in Mechanical Engineering (B.tech), in the year 2012. After that he has worked as lecturer in Aryan Institute of Technology in Ghaziabad, Uttar Pradesh in the year 2012-2013. In the year 2013, he joined in the Master of Engineering (CAD/CAM Engineering) Programme at Thapar University, Patiala, Punjab. His ME thesis work is in the Bond Graph Aided Thermal Analysis of Finite Journal Bearing.